Sea ice feedback and Cenozoic evolution of Antarctic climate and ice sheets

Robert DeConto,[1] David Pollard,[2] and David Harwood[3]

Received 27 July 2006; revised 24 February 2007; accepted 20 March 2007; published 24 August 2007.

[1] The extent and thickness of Antarctic sea ice have important climatic effects on radiation balance, energy transfer between the atmosphere and ocean, and moisture availability. This paper explores the role of sea ice and related feedbacks in the Cenozoic evolution of Antarctic climate and ice sheets, using a numerical climate model with explicit, dynamical representations of sea ice and continental ice sheets. In a scenario of decreasing Cenozoic greenhouse gas concentrations, our model initiates continental glaciation before any significant sea ice forms around the continent. Once variable ice sheets are established, seasonal sea ice distribution is highly sensitive to orbital forcing and ice sheet geometry via the ice sheet's control on regional temperature and low-level winds. Although the expansion of sea ice has significant climatic effects near the coast, it has only minimal effects in the continental interior and on the size of the ice sheet. Therefore the Cenozoic appearance of Antarctic sea ice was primarily a response to the growth of grounded ice sheets and was not a critical factor in episodes of Paleogene and Neogene glaciation. The influence of the East Antarctic Ice Sheet on sea ice, Southern Ocean surface temperatures, and winds has important implications for ocean circulation, the marine carbon cycle, and the development of the West Antarctic Ice Sheet. The sensitivity of sea ice to grounded ice sheets implies reconstructions of sea ice based on marine diatoms are good indicators of glacial conditions in the continental interior and may provide insight into the long-term stability of Antarctic Ice Sheets.

Citation: DeConto, R., D. Pollard, and D. Harwood (2007), Sea ice feedback and Cenozoic evolution of Antarctic climate and ice sheets, *Paleoceanography*, *22*, PA3214, doi:10.1029/2006PA001350.

1. Introduction

[2] The maximum equatorward extent and thickness of Southern Hemisphere sea ice varies over a wide range of timescales, with important climatic effects on albedo, energy transfer between the ocean and atmosphere, regional moisture availability, air-sea gas exchange, and deep water formation [*Bromwich et al.*, 1998b; *Fletcher*, 1969; *Liu et al.*, 2002; *Rind et al.*, 1995; *Stephens and Keeling*, 2000; *Washington and Meehl*, 1996]. Today, sea ice reaches ~55°S in the South Atlantic and ~60°S in the South Pacific during September–October, covering an area about 20×10^6 km^2. Sea ice cover decreases to ~4×10^6 km^2 in February–March, with perennial cover (the area maintaining >30% fractional coverage) averaging between ~$1.5–2.0 \times 10^6$ km^2 [*Parkinson*, 1998].

[3] In today's world, interannual-decadal Antarctic sea ice variability on the order of ~14,000 km^2 yr^{-1} [*Zwally et al.*, 2002] has been correlated with El Niño Southern Oscillation (ENSO) and the Antarctic Oscillation via a wide range of possible linkage mechanisms associated with surface heat flux anomalies, clouds, mean meridional atmospheric circulation, heat flux, and sea ice advection [*Carleton*, 1989; *Carleton*, 2003; *Liu et al.*, 2004]. Over glacial-interglacial timescales, sea ice reconstructions based on diatom assemblages show much larger variability [*Armand*, 2000; *Cooke and Hays*, 1982; *Gersonde et al.*, 2005]. Equatorward extent of Southern Ocean sea ice at the Last Glacial Maximum (LGM) is thought to have increased between 5° and 8° [*Crosta et al.*, 1998], effectively doubling its area relative to today, while substantially reduced sea ice is evident during other periods of the Pleistocene and Pliocene [*Bohaty et al.*, 1998; *Mahood and Barron*, 1996; *Whitehead et al.*, 2005; *Winter and Harwood*, 1997].

[4] On longer timescales, paleo-Global Climate Model (GCM) simulations (like those shown here) suggest Southern Hemisphere sea ice was absent during peak warm periods of the Mesozoic and Cenozoic. However, the presence of sea ice in the Late Cenozoic and its dramatic expansion during peak Quaternary glacial periods suggests the possibility of at least some sea ice during relatively cold episodes of Antarctic ice sheet expansion in the Paleogene and Neogene (for example, Oi-1, Mi-1-4) [*Billups and Schrag*, 2002; *Lear et al.*, 2000; *Miller et al.*, 1987; *Zachos et al.*, 2001a]. Considering the powerful albedo/cooling feedback associated with sea ice, its growth around the Antarctic margin could have played an active role in these and other episodes of cooling and glaciation. Sea ice-ice sheet linkages could also be important during warming events. For example, ice margin retreat in the Lambert/Prydz Bay region [*Hambrey and McKelvey*, 2000a; *Whitehead et al.*, 2005] is coincident with Pliocene intervals of minimal sea ice and

[1]Department of Geosciences, University of Massachusetts, Amherst, Massachusetts, USA.
[2]Earth and Environmental Systems Institute, Pennsylvania State University, University Park, Pennsylvania, USA.
[3]Department of Geosciences, University of Nebraska-Lincoln, Lincoln, Nebraska, USA.

0883-8305/07/2006PA001350$12.00

elevated sea surface temperatures (SSTs) [*Harwood et al.*, 2000; *Whitehead and Bohaty*, 2003; *Whitehead et al.*, 2001], although a clear cause-and-effect relationship has yet to be determined.

[5] The climatic effects of Antarctic sea ice variability have been studied extensively from both observational and climate-modeling perspectives [*Bromwich et al.*, 1998a; *Gloerson*, 1995; *Ingram et al.*, 1989; *Jeffries*, 1998; *Liu et al.*, 2003; *Simmonds and Budd*, 1991; *Weatherly*, 2004; *Wu et al.*, 1996]. These and other studies have shown that changes in Antarctic sea ice do indeed produce strong regional climate effects that can extend into the tropics and even the Northern Hemisphere via teleconnections associated with clouds, the forcing of stationary planetary waves, cyclogenesis, and storm track location [*Bromwich et al.*, 1998a; *Carleton*, 2003; *Lubin et al.*, 1998; *Simmonds and Jacka*, 1995]. Over interannual and longer timescales, the effects of Antarctic sea ice include the well-known sea ice-albedo feedback mentioned above, whereby cooler climates produce sea ice which increases albedo and reduces net radiation, leading to additional cooling and more sea ice. In coupled atmosphere-ocean GCM (A/OGCM) simulations of the LGM [*Shin et al.*, 2003], expanding seasonal sea ice strengthens the westerlies. Increased equatorward Ekman transport reduces poleward oceanic heat transport and drives the sea ice edge northward, adding to the cooling/albedo feedback.

[6] Like albedo, the insulating effect of sea ice on surface air temperature and moisture availability also has important implications for polar (and possibly global) climate. Modern observations have shown that ocean-atmosphere heat exchange can be orders of magnitude smaller over sea ice than adjacent open-water locations and polynas [*Andreas and Murphy*, 1986; *King and Turner*, 1997], where local heat flux can exceed 500 Wm^{-2} [*Fahbach et al.*, 1994]. Over ice-free regions, atmospheric heating and moisture flux are known to affect regional pressure and precipitation patterns [*Bromwich et al.*, 1998a; *Parkinson et al.*, 2001]. In the Northern Hemisphere, sea ice variability and associated changes in moisture availability have been implicated in hysteresis between sea ice and Quaternary ice sheets, with land ice growing when sea ice is reduced and shrinking when sea ice is more extensive [*Sayag et al.*, 2004]. In the Southern Hemisphere, GCM experiments using modern boundary conditions have shown that reductions in sea ice significantly increase precipitation (up to 100%) over previously ice-covered regions and in coastal locations but with much smaller effects on the continental ice sheet, where increased moisture convergence is approximately balanced by increased evaporation [*Weatherly*, 2004].

[7] At times in the geologic past, when global mean temperatures were warmer and Antarctic ice sheets were smaller than today, the net effect of expanding sea ice on continental snow budgets was likely a complex balance between albedo-enhanced cooling, particularly in coastal and lower-altitude locations susceptible to high-ablation rates during austral summer, and reductions in moisture availability and snowfall in the continental interior. During times of sea ice retreat and warmer SSTs, increased moisture availability should increase total precipitation [*Oglesby*, 1989; *Prentice and Mathews*, 1991]. However, warming can also increase the fraction of precipitation falling as rain [*Simmonds and Budd*, 1991], so the net effect of sea ice cover on Antarctic ice sheet development and Cenozoic variability remains unclear. While the problem is well-suited to numerical climate modeling, most prior work has focused on positive sea ice-albedo feedback in future global warming scenarios [*Pollard and Thompson*, 1994; *Rind et al.*, 1995], or the effects of open water on the present-day climate system [*Bromwich et al.*, 1998a; *Simmonds and Budd*, 1991; *Weatherly*, 2004; *Wu et al.*, 1996]. However, model results using modern boundary conditions may not be applicable to ancient climates when the Antarctic ice sheet was nonexistent or smaller than today. Today's Antarctic continental elevations (>2000 m) and steep coastal topographic slopes limit the climatic effects (particularly the advection of moisture) in the interior, so the effects of sea ice on glacial mass balance may have been larger during intervals of the Cenozoic when ice sheets were small. Furthermore, the area for sea ice expansion around Antarctica is essentially unlimited, so the strength of positive sea ice feedback should be larger for a cooling climate than a warming climate [*Rind et al.*, 1995]. This positive (cooling) ice/albedo feedback may have played an important role in the sudden climate events recognized during the Paleogene and Neogene as the planet transitioned from a greenhouse to icehouse world.

[8] This paper addresses the role of sea ice in the climatic and glacial evolution of the Antarctic region through the Cenozoic, including the sometimes sudden variations in the Cenozoic ice volume inferred from benthic marine oxygen isotope and Mg/Ca records [*Billups and Schrag*, 2003; *Coxall et al.*, 2005; *Holbourn et al.*, 2005; *Lear et al.*, 2000; *Lear et al.*, 2004; *Miller et al.*, 1987; *Zachos et al.*, 2001a]. We use a GCM with explicit, dynamical representations of sea ice and grounded continental ice sheets to test (1) the sensitivity of Southern Hemisphere sea ice to early Cenozoic climate forcing (atmospheric CO_2, orbital variability, and ice sheet configuration) and (2) the importance of physical sea ice-atmosphere feedbacks on the climatic and glacial evolution of the Antarctic interior.

2. Numerical Model Simulations

2.1. Model Description

[9] As in our coupled GCM-ice sheet modeling work of the Paleogene [*DeConto and Pollard*, 2003a; *DeConto and Pollard*, 2003b] we use the GENESIS Version 2.2 GCM, which includes several improvements for simulating realistic snow mass balances over ice sheets [*Pollard and Thompson*, 1997; *Thompson and Pollard*, 1997]. The performance of GENESIS has been studied extensively, with an emphasis on the cryosphere [*Pollard and Thompson*, 1994; *Pollard and Thompson*, 1997; *Thompson and Pollard*, 1997]. Present-day seasonal sea ice distributions and snow mass balances over Antarctica and Greenland simulated by GENESIS are among the most realistic of paleoclimatic GCMs [*Pollard*, 2000], and the model has been used in a number of paleoclimate simulations of Laurentide [*Pollard and Thompson*, 1997] and Antarctic ice sheet variability

Table 1. Model Simulations and Relevant Model Inputs

Number	CO_2 Mixing Ratio[a]	Orbital Parameters (ecc., obl., pre.)[b]	Ice Sheet Geometry[c]
1	$2 \times CO_2$	0.05, 22,5, 270.0	NOICE
2	$2 \times CO_2$	0.0, 23.5, 0.0	NOICE
3	$2 \times CO_2$	0.05, 24.5, 90.0	NOICE
4	$2 \times CO_2$	0.05, 22,5, 270.0	MEDICE
5	$2 \times CO_2$	0.0, 23.5, 0.0	MEDICE
6	$2 \times CO_2$	0.05, 24.5, 90.0	MEDICE
7	$2 \times CO_2$	0.05, 22,5, 270.0	FULLICE
8	$2 \times CO_2$	0.0, 23.5, 0.0	FULLICE
9	$2 \times CO_2$	0.05, 24.5, 90.0	FULLICE
10	$3 \times CO_2$	0.05, 22,5, 270.0	NOICE
11	$3 \times CO_2$	0.0, 23.5, 0.0	NOICE
12	$3 \times CO_2$	0.05, 24.5, 90.0	NOICE
13	$3 \times CO_2$	0.05, 22,5, 270.0	MEDICE
14	$3 \times CO_2$	0.0, 23.5, 0.0	MEDICE
15	$3 \times CO_2$	0.05, 24.5, 90.0	MEDICE
16	$3 \times CO_2$	0.05, 22,5, 270.0	FULLICE
17	$3 \times CO_2$	0.0, 23.5, 0.0	FULLICE
18	$3 \times CO_2$	0.05, 24.5, 90.0	FULLICE

[a]CO_2 mixing ratios in multiples of the preindustrial level of 280 ppmv [*Houghton et al.*, 1990].
[b]Idealized orbital parameters producing relatively cold, moderate, or warm austral summers. Values of precession are shown as the prograde angle between perihelion and the Northern Hemisphere vernal equinox.
[c]Prescribed ice sheet configurations representing an ice-free, partly glaciated, and fully glaciated East Antarctica as shown in Figure 1.

[*DeConto and Pollard*, 2003a; *DeConto and Pollard*, 2003b; *Pollard and DeConto*, 2005].

[10] The atmospheric component of GENESIS has 18 vertical layers and a spectral resolution of T31 ($\sim 3.75^\circ \times 3.75^\circ$), coupled to $2^\circ \times 2^\circ$ surface model components including a nondynamical 50-meter slab ocean, a dynamic-thermodynamic sea ice model, and multilayer models of soil, snow, and vegetation. Sea-surface temperatures are calculated by the model and are freely varying. Similarly, ocean heat transport is not prescribed but is calculated as linear diffusion down the local ocean temperature gradient, with the diffusion coefficient depending on latitude and the zonal fraction of land versus sea. Modifications to the standard GENESIS version 2.0 [*Thompson and Pollard*, 1997] include improvements in the slab ocean model, yielding more realistic present zonal ocean heat transport within the range of uncertainties of observations and like those produced by GCMs with dynamical, full-depth oceans (with about 1.5 and 2.0 petawatts peak heat transport in the southern and northern hemisphere, respectively), and the elimination of hard-coded hemispheric asymmetries in cloud single-scattering albedo. While the use of a slab ocean component precludes explicit examination of sea ice effects on the thermohaline circulation, its computational efficiency allows multiple sensitivity tests using different ice sheet configurations, CO_2, and orbital parameters, while fully accounting for feedbacks between the surface ocean, sea ice, and our dynamic ice sheet model.

[11] Model components representing snow, sea ice, and grounded ice are of particular importance to this study. The three-layer snow model represents snow cover on soil, ice sheets, and sea ice surfaces, accounting for fractional areal cover where snow is thin. Heat is diffused linearly through the snow, with the total thickness changing as a function of additional snowfall or melting on the upper layer. Fractional snow cover is diagnosed from total snow mass assuming a linear relationship between fraction and depth below 100% cover. The depth at which the cover reaches 100% varies within the range 20 to 70 cm depending on the height of the lower vegetation canopy, which in this case is prescribed as tundra over ice-free regions of Antarctica. Solar albedos of melting snow and ice sheet surfaces for the visible and near-infrared wave bands are 0.55 and 0.35 for snow (except on land ice), 0.70 and 0.55 for land ice and associated snow cover, and 0.70 and 0.40 for sea ice, respectively. For colder snow between 0 and -5°C, albedos of snow and ice surfaces increase linearly. Below -5°C, the values are 0.90 and 0.60 for snow and 0.80 and 0.50 for sea ice. These albedos are used equally for direct and diffuse beams, except for the direct beam on snow, which depends on solar zenith angle. The effects of snow compactness, aging, and moisture content on albedo are ignored.

[12] In the natural world, sea ice formation depends on ocean temperature and heat flux, and its spatial distribution is affected by wind stress, inertial forces, and ocean currents. Our three-layer sea ice thermodynamic model predicts the local melting and freezing of sea ice, essentially as in [*Semtner*, 1976]. Fractional areal cover is accounted for as in the studies of *Hibler* [1979] and *Harvey* [1988]. While our slab-ocean component lacks explicit representation of ocean currents, GCM surface winds drive the sea ice dynamics, with advection simulated as a cavitating fluid [*Flato and Hibler*, 1990; *Flato and Hibler*, 1992]. In this case, the ice resists compressive stresses but offers no resistance to divergence or shear. In addition to its effect on albedo, snow cover increases the conductive insulation potential of sea ice, reduces the thickening rate of the underlying ice, and decreases surface roughness [*Ledley*, 1991; *Sturm et al.*, 1998]. In the slab-ocean configuration used here, the GCM reaches equilibrium within the first 15 years of each simulation. All GCM results are shown as averages over the last 10 years of 30-year simulations, so variables including sea ice fraction and thickness are spun up and in climatic equilibrium.

[13] To test the long-term effects of different GCM climates on ice sheet development, the GCM is coupled to

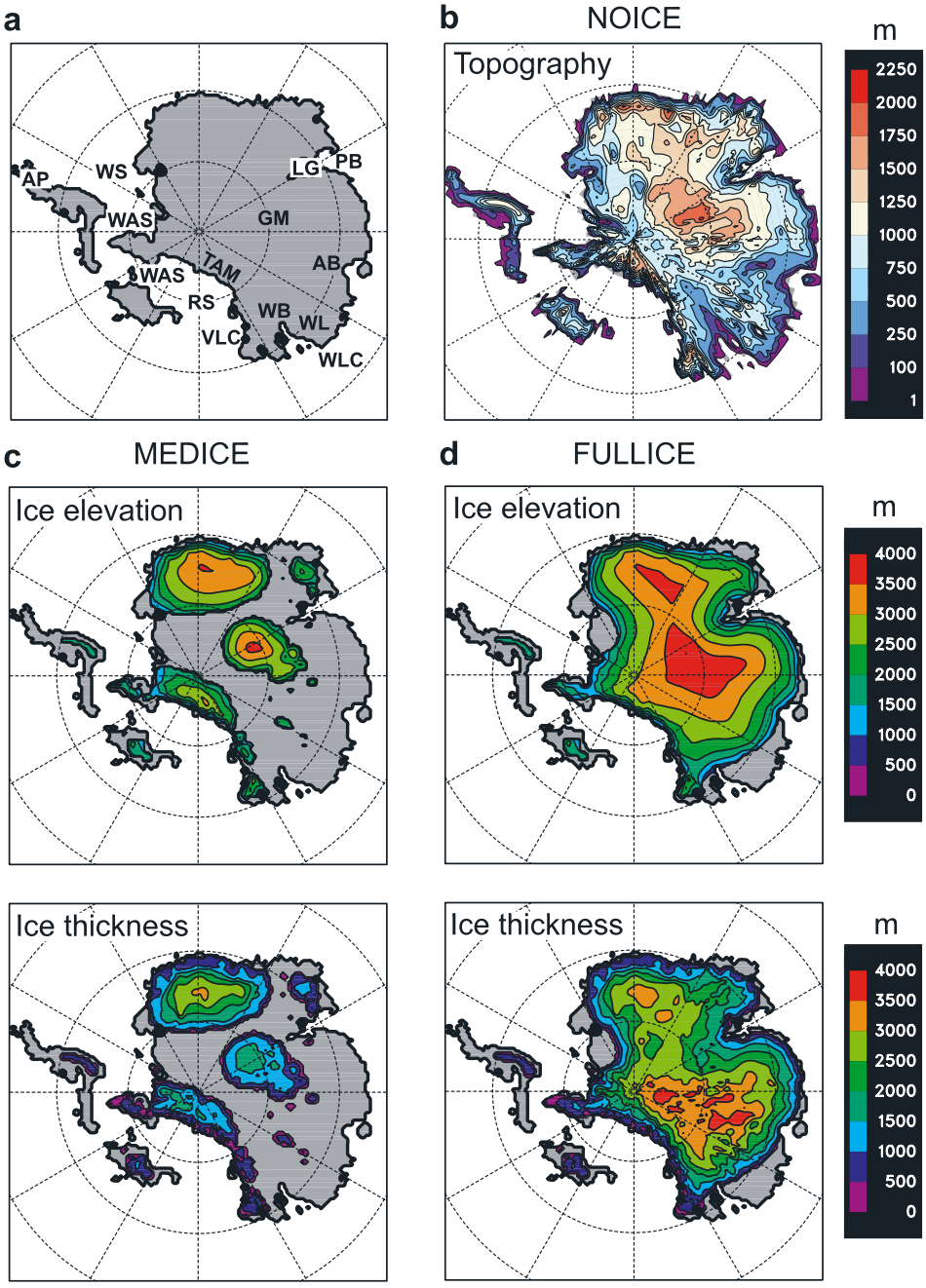

Figure 1. Antarctic paleogeography and ice sheet geometries used in our Paleogene GCM simulations. (a) Place names used in the text include: AP, Antarctic Peninsula; AB, Aurora Basin; GM, Gamburtsev Mountains; LG, Lambert Graben; RS, Ross Sea; TM, Transantarctic Mountains; VLC, Victoria Land coast; WAS, West Antarctic Seaway; WB, Wilkes Basin; WL, Wilkes Land; WLC, Wilkes Land coast. (b) NOICE; Ice-free elevation (meters above sea level) based on isostatically relaxed present-day bedrock elevations (see text). (c) Partially (MEDICE) and (d) fully glaciated (FULLICE) Antarctic ice sheet geometries, elevations, and thicknesses (in meters), from prior coupled GCM-dynamical ice sheet model simulations [*DeConto and Pollard*, 2003a].

a standard three-dimensional thermomechanical ice sheet model [*Huybrechts*, 1990; *Huybrechts*, 1993; *Ritz et al.*, 1997], modified to allow asynchronous coupling with the GCM [*DeConto and Pollard*, 2003a]. The ice sheet component predicts the evolution of grounded ice in response to surface mass-balance forcing, ice flow, and basal melting. Ice flow is mainly by shear under its own weight, following the shallow ice approximation. The ice sheet grid is polar stereographic with 40 $\times$ 40 km resolution and ten unequally spaced vertical layers. An alternating direction-implicit

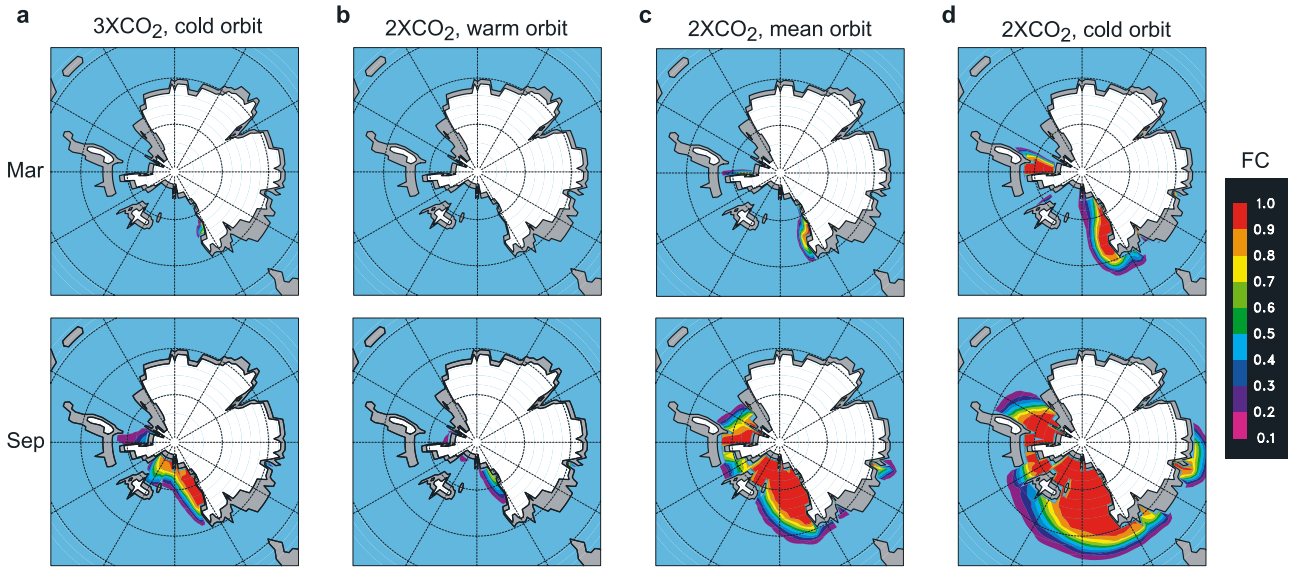

Figure 2. Simulated sea ice fractional cover (FC) during March (top) and September (bottom) with the FULLICE ice sheet configuration shown in Figure 1, different levels of atmospheric CO_2, and different orbital configurations (see Table 1). (a) Seasonal sea ice with $3 \times CO_2$, the cold orbital case, and FULLICE. At $3 \times CO_2$, no seasonal sea ice forms in the MEDICE or NOICE cases (not shown). (b) Seasonal sea ice cover with FULLICE, $2 \times CO_2$, and the warm orbital case; (c) FULLICE, $2 \times CO_2$, and the medium orbital case; and (d) FULLICE, $2 \times CO_2$, and the cold orbital case. No seasonal sea ice forms in the NOICE and MEDICE cases with $2 \times CO_2$ and warm or mean orbits (not shown).

numerical scheme is used, with time-implicit tridiagonal Newton-Raphson contributions from all terms, allowing a 10-year timestep. Thermodynamic equations are solved to account for ice temperature's effect on deformation and basal conditions. Temperatures through the ice sheet are affected by surface temperature, advection, vertical diffusion, frictional heating, and geothermal heat flux. Vertical diffusive temperatures are predicted through the upper 2 km of underlying bedrock using a six-layer model and a uniform geothermal heat flux of 41 mWm^{-2}. The asthenospheric response to ice load is a simple local relaxation toward isostacy, with a timescale of 5000 years. Lithospheric response is modeled as linear elastic deformation [*Brotchie and Sylvester*, 1969] using a flexural rigidity of 1×10^{25} N m [*Huybrechts*, 1990]. There is no explicit representation of ice shelves in this model and all ice reaching the coast calves instantaneously, so the development of ice shelves between West and East Antarctica is not directly simulated. In reality, ice shelves can only be initiated if (1) grounded ice reaches the coast, and (2) regional climate is cold enough to avoid strong surface or basal melt (i.e., probably cold enough to maintain perennial sea ice). Because our model predicts these two conditions, some inferences concerning ice shelves can be made.

2.2. Effect of Continental Ice on Seasonal Sea Ice Extent

[14] To explore the effects of Paleogene Antarctic ice sheet variations on sea ice, we ran a suite of eighteen climate simulations (Table 1) using the GCM described above, a 34-Ma global paleogeography, combinations of $2\times$ or $3\times$ atmospheric CO_2 ($1 \times CO_2 = 280$ ppmv), three different orbital configurations, and prescribed ice sheet geometries representing unglaciated (NOICE), moderately glaciated (MEDICE), and a fully glaciated (FULLICE) East Antarctica (Figure 1). The global 34-Ma paleogeography is the same as that used in our prior simulations of Paleogene climates and ice sheets [*DeConto and Pollard*, 2003a] and includes reconstructions of earliest Oligocene shorelines, topography, and vegetation superposed on a global tectonic model [*Hay et al.*, 1999] and rotated to their 34-Ma positions. Ice-free Antarctic topography (Figure 1b) is reconstructed from a modern 5-km digital ice surface and bedrock elevation data [*Bamber and Bindschadler*, 1997], isostatically relaxed to ice-free equilibrium, while accounting for higher, ice-free sea level. The prescribed ice sheet geometries (Figures 1c and 1d) come from our prior coupled GCM-ice sheet simulations of East Antarctic glaciation in the earliest Oligocene [*DeConto and Pollard*, 2003a; *DeConto and Pollard*, 2003b]. Because there are no explicit ice shelves in these simulations, the flooded region between East and West Antarctica (West Antarctic Seaway) is initialized as open water.

[15] To simplify this paper, we show the results from selected simulations, all with $2 \times CO_2$ (except in Figure 2a). Higher CO_2 mixing ratios were found to produce only limited seasonal sea ice regardless of ice sheet size or orbital configuration. Additionally, prior work [*DeConto and Pollard*, 2003b] showed that $3 \times CO_2$ is above this GCM's threshold value for initiating Antarctic glaciation. Figure 2 shows maximum and minimum (March and September) sea ice cover averaged over the last 10 years of 30-year GCM integrations, with different combinations of atmospheric CO_2 and orbital parameters representing

cold (eccentricity = 0.05; obliquity = 23.5°; perihelion in July), moderate (eccentricity = 0; obliquity = 23.5°), warm (eccentricity = 0.05; obliquity = 24.5°; perihelion in January) Antarctic summer climates, and prescribed ice sheet sizes. At 3 × CO_2, limited seasonal sea ice forms adjacent to the Victoria Land coast and only with a large continental ice sheet and cold austral summer orbit (Figure 2a). At 2 × CO_2, seasonal sea ice extent is sensitive to both prescribed orbital parameters and ice sheet configuration. With the 'warm' orbital parameters, a relatively small area of ice cover forms along the Victoria Land coast, but only in the FULLICE case, and no sea ice forms with the warm orbital parameters and the smaller MEDICE and NOICE ice sheet configurations. With the exception of the three fixed ice sheet geometries shown in Figure 1, the simulations shown in Figure 3 use identical initial and boundary conditions. This approach isolates the effects of growing continental ice sheets on sea ice extent. As clearly seen in Figure 3, sea ice extent and thickness are highly dependent on continental ice sheet geometry. In the MEDICE case, austral winter sea ice expands markedly relative to the NOICE case, filling most of the shallow West Antarctic Seaway. A small area of perennial sea ice is maintained along the Victoria Land coast, marginal to the glaciated Transantarctic Mountains. In the FULLICE case, late-winter sea ice extends to ~65°S around much of the continent, particularly in the Ross Sea sector. The area of perennial sea ice also expands along the Victoria Land coast and in the Weddell Sea region. In the FULLICE simulations, sea ice reaches maximum thickness late in austral winter. The thickest ice is concentrated in the Ross Sea, along the Northern Victoria Land coastline, and against the peninsula extending northward from the South Pole on the Antarctic Peninsula side of the West Antarctic Seaway.

[16] The effects of growing ice sheets on Southern Hemisphere seasonal temperature are shown in Figure 4. Winter surface air temperatures over the West Antarctic Seaway (ocean grid cells) fall from just below freezing in the NOICE case, to −15 to −20°C in the FULLICE scenario, with the area within the zero degree isotherm expanding equatorward to ~65°S. Seasonal temperature differences between the FULLICE and NOICE case are shown in Figure 5, showing that the direct effects of a large continental ice sheet on austral winter temperatures exceed 10°C over a significant fraction of the Southern Ocean, with the perturbation to mean annual temperature extending to ~50°S (Figure 5b). While an in-depth discussion of the global atmospheric effects of a growing Antarctic ice sheet will be the focus of another paper, we note the addition of the FULLICE ice sheet reduces global and Southern Hemispheric mean annual temperatures by 0.8°C and 1.5°C, respectively. With the addition of the ice sheet, the low-level polar high strengthens and the circumpolar trough stays close to 65°S but deepens, increasing the intensity of the westerlies over most of the Southern Ocean poleward of 55°S.

[17] The growing ice sheet's influence on the development of the katabatic-dominated Antarctic wind field is clearly seen in Figure 6. In the MEDICE and FULLICE simulations, a combination of katabatic forcing (radiational and diabatic cooling) and topographic modification of the large-scale circulation creates strong winds down steep topographic gradients and in troughs between elevated terrain and ice caps. Southeasterly outflow dominates most of the circum-Antarctic margin, with coastal and offshore wind speeds averaging over 10 m s^{-1} in many locations. The large ice sheet also affects the dynamics of the free atmosphere, increasing the intensity of the circumpolar vortex and displacing the center of 500 hPa cyclonic circulation slightly eastward, away from the pole and toward the geographic center of East Antarctica.

[18] Comparison of Figure 3 with Figures 4 and 6 shows the effects of ice sheet geometry on the extent and distribution of sea ice via its combined control on surface temperature and the polar wind field. In the FULLICE simulation, thick (>5 m) accumulations of sea ice converge along the northern Victoria Land coastline in response to the strong southerly flow adjacent to the Victoria Land coast and the Transantarctic Mountains. Winter winds provide easterly wind stress across the Weddell Sea, pushing sea ice against the Antarctic Peninsula where thick, perennial ice cover is maintained.

2.3. Sea Ice Effect on Ice Sheet Mass Balance

[19] In the GCM sensitivity experiments described above, the distribution of ice in the continental interior is shown to have an important effect on the maximum seasonal extent, fractional cover, seasonal duration, and thickness of the sea ice surrounding the continent. In those simulations, Southern Ocean sea ice is considered part of the fast-response (seasonal) climate system, and the grounded Antarctic ice is a long-term (10^3–10^4 years) component that is assumed to be invariant over the decadal timescales of our GCM simulations.

[20] Here we test the impact of sea ice on continental climate, particularly net snow accumulation (surface mass balance), and the importance of sea ice-related feedbacks versus other purely atmospheric and/or open-ocean influence on ice sheet variability. To assess sea ice feedback, we compare simulations with sea ice feedback (allowing freely varying, prognostic sea ice as shown above) with a simulation without sea ice feedback (with sea ice prescribed and fixed). To do this, we performed another 2 × CO_2 GCM simulation (MINSEAICE) with the same continental-scale ice sheet as in our FULLICE simulation (Figure 3, right panels) but with sea ice prescribed and fixed from the monthly geographical extents in the prior experiment with no ice sheet (NOICE) and only minimal predicted sea ice during austral winter (Figure 3, left panels). In all ice-free grid points in the MINSEAICE run, SSTs are predicted by the slab-ocean component of the GCM as usual. If SSTs fall to the freezing point where no sea ice is prescribed, the sea surface is forced to remain unfrozen at −1.9°C. Assuming our results do not depend on the details of sea ice lead fractions and thicknesses [*Andreas and Murphy*, 1986], we simply set them to constant values of 10% and 1 m, respectively; similar to but not exactly their values in the first run. By comparing model results with minimal fixed sea ice with those when sea ice is predicted and freely varying as in the FULLICE simulation, we can isolate the magnitude of sea ice feedback in a scenario of continental glaciation.

[21] The simulated effects of circum-Antarctic sea ice expansion in the FULLICE simulation (Figure 2d), hence-

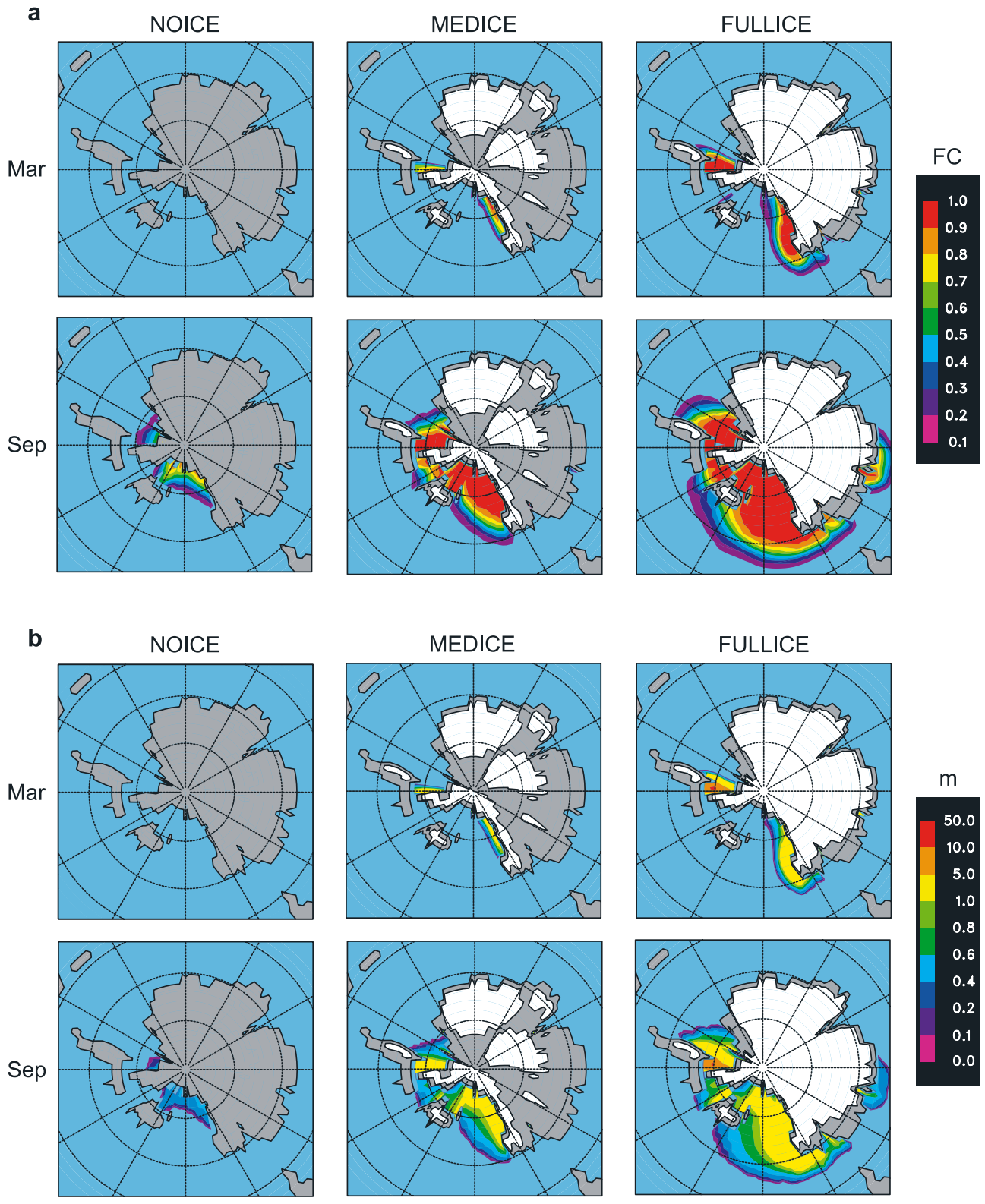

Figure 3. Sea ice extent with NOICE, MEDICE, and FULLICE ice sheet configurations (left to right) and the cold austral summer orbital parameters described in the text and in Table 1. With the exception of ice sheet geometry, boundary conditions are identical in the three simulations, isolating the influence of grounded ice volume on seasonal sea ice. (a) March (top) and September (bottom) fractional cover and (b) corresponding sea ice thickness in meters.

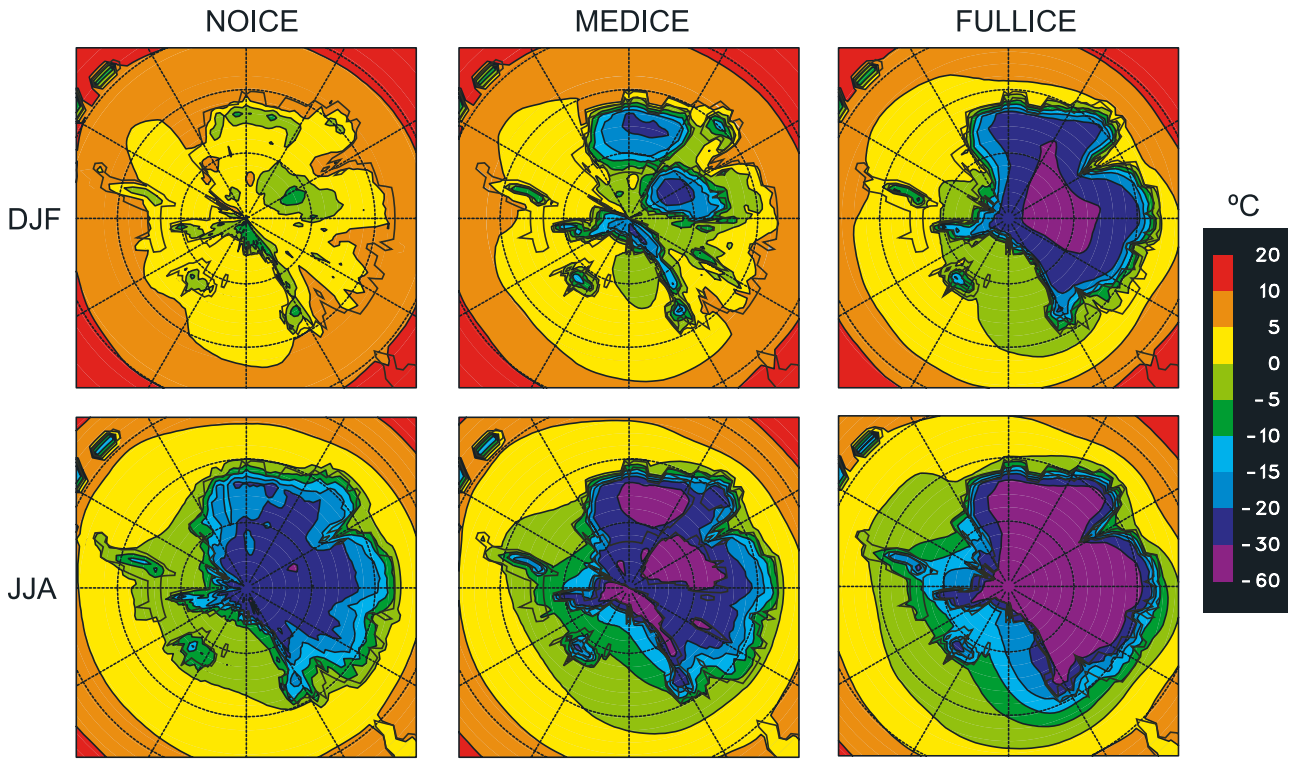

Figure 4. Surface (2 m) seasonally averaged temperatures; December, January, July (top); June, July, August (bottom) for the three ice sheet geometries as in Figures 2d and 3.

forth called MAXSEAICE, versus the mostly open-ocean conditions in the MINSEAICE run are directly related to the increase in albedo and reductions in sensible and latent heat flux over the sea ice zone. As expected, albedo over the sea ice covered region increases dramatically (approaching 0.9) where fractional sea ice cover is greater than 0.8 and the effects of snow cover come into play. The growth of sea ice versus forced open-water conditions decreases both upward sensible and latent heat flux in the sea ice zone by as much as 60 and 40 W m^{-2}, respectively (Figure 7). This result is generally consistent with the results of *Bromwich et al.* [1998a, 1998b] in their experiments using the National Center for Atmospheric Research (NCAR) Climate Chemistry Model 2 (CCM2) GCM and present-day climate as the control, with sea ice removed as in our MINSEAICE case.

[22] Figure 8 shows the overall climatic effect of sea ice expansion around the continent as the difference between the MAXSEAICE case with prognostic sea ice (FULLICE; Figures 2d and 3) and the MINSEAICE case described above. As expected, the effect on temperature (Figure 8a) is greatest during austral winter, when sea ice extent is greatest and the insulating effect on upward heat flux is at a maximum (Figure 7). As with heat flux, the largest temperature differences are over the Western Antarctic Seaway, the subaerial West Antarctic archipelago, and along the northern Victoria Land and Wilkes Land coastlines, where winter temperatures are reduced by 10°–15°C. Despite these dramatic regional effects, significant continental cooling is mostly limited to the lower elevations of the Victoria Land margin and West Antarctica, with some warming (<2°C) over parts of the interior (Figure 8). Again, these results are similar to those shown in prior GCM simulations of modern climate with forced open water around Antarctica [*Bromwich et al.*, 1998a; *Weatherly*, 2004; *Wu et al.*, 1996], with the primary exception being the extent of the temperature change propagating over some land areas, which is generally greater in our simulations. This is likely due to the smaller Paleogene ice sheet, which does not intersect the coastline everywhere and has shallower topographic slopes than the present ice sheet.

[23] Like temperature, statistically significant changes in precipitation are mostly limited to the sea ice zone. The greatest changes occur during austral winter over the West Antarctic Seaway, where the localized decrease in atmospheric moisture and surface heating reduces both stratiform and convective precipitation by a total of ~1.5 mm day^{-1}. Precipitation decrease is concentrated along the Transantarctic Mountains, where the adjacent moisture source for orographically forced precipitation is eliminated. A decrease in precipitation on the East Antarctic margin near the present-day Aurora Basin is located adjacent to an isolated zone of winter sea ice accumulation. The propagation of anomalies into the interior is mostly limited to regions adjacent to thick sea ice and in lower elevations where the ice sheet is either absent or thin and fractional.

[24] Simulated sea level pressure for MAXSEAICE, MINSEAICE, and the differences between them are shown in Figure 9. The expansion of sea ice and associated effects

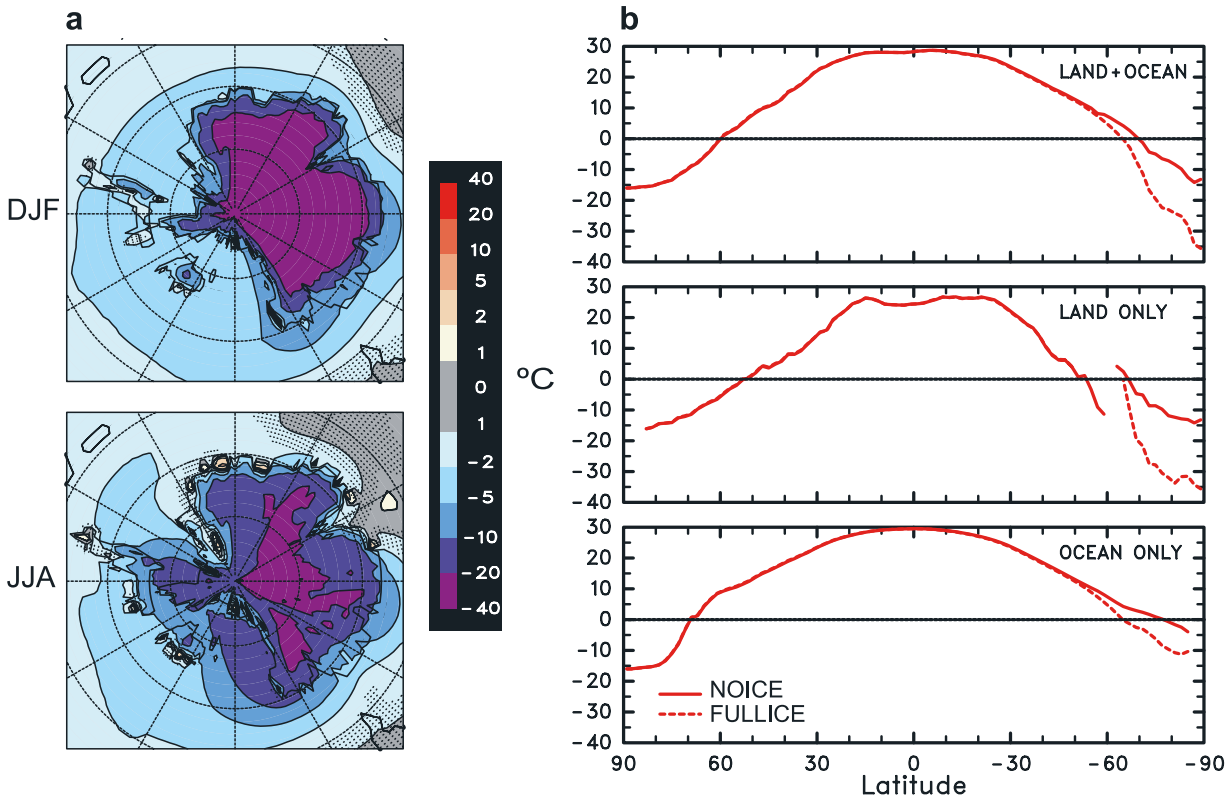

Figure 5. Seasonally averaged surface (2 m) temperature difference (a) between the simulation with no Antarctic ice sheet (NOICE) and a fully glaciated East Antarctica (FULLICE). (b) Annual zonal mean temperature with NOICE (solid line) and the FULLICE ice sheet (dashed line) over all grid points (top), over land only (middle), and over ocean only (bottom). The poleward jump in zonal land temperatures at 60°S reflects the lower prescribed elevations on the Antarctic Peninsula, relative to the Southern Andes.

on the surface boundary layer deepens the polar trough. During austral summer, zonal mean surface pressure decreases by ~3 hPa in the trough and over much of the continent. Sea level pressure increases by a nearly equal amount over the Southern Ocean equatorward of ~60°S, strengthening the low-level westerlies. Seasonal positions of three dominant low-pressure centers and high-pressure ridges are displaced zonally, and the lows in the South Pacific and South Atlantic deepen significantly. While the shifting pressure patterns, winds, and storm tracks affect the distribution of maximum precipitation along the coast and equatorward of the direct influence of the katabatic outflow, precipitation changes over most the continental interior are generally below the level of statistical significance (Figure 8b), suggesting the effects on mass balance over an established ice sheet would be small.

[25] To examine the total climate effects of sea ice on glacial mass balance over an existing ice sheet, we isolate snowfall from the total precipitation field (Figure 10). As expected, the difference pattern closely follows that of total precipitation, with the biggest changes centered over the West Antarctic Seaway and the Wilkes Land margin of East Antarctica. While the total area with snowfall greater than 1.0 mm day^{-1} is larger in the MAXSEAICE case, reflecting the equatorward shift of the zero degree isotherm, the area of snowfall rate greater than 1.5 mm day^{-1} is larger in the MINSEAICE case, particularly over the West Antarctic Seaway and along the western side of the Transantarctic Mountains. As with total precipitation, simulated changes in snowfall over the continental interior are generally small and statistically insignificant. While smaller than today's East Antarctic Ice Sheet (EAIS), our prescribed Paleogene ice sheet is still capable of limiting most precipitation to the coast and lower elevations of the ice sheet flanks, with little snowfall reaching the interior plateau (Figures 10a and 10b), regardless of proximity to open water. While medium-resolution, spectral GCMs are known to produce biases in precipitation in areas of steep topographic relief, such as along the flanks of mountain ranges and ice sheets, our GCM produces realistic glacial mass balances over the modern ice sheet [*Thompson and Pollard*, 1997]. Furthermore, the Paleogene ice sheet used as a boundary condition in these simulations has a considerably lower profile than the modern ice sheet, mitigating the spectral truncation problem.

2.4. Ice Sheet Model Simulations

[26] To better determine the effect of sea ice on the long-term (>10^4 years) evolution of the EAIS, we forced our ice sheet model with surface mass balance forcing with both MAXSEAICE and MINSEAICE climatologies. Differences

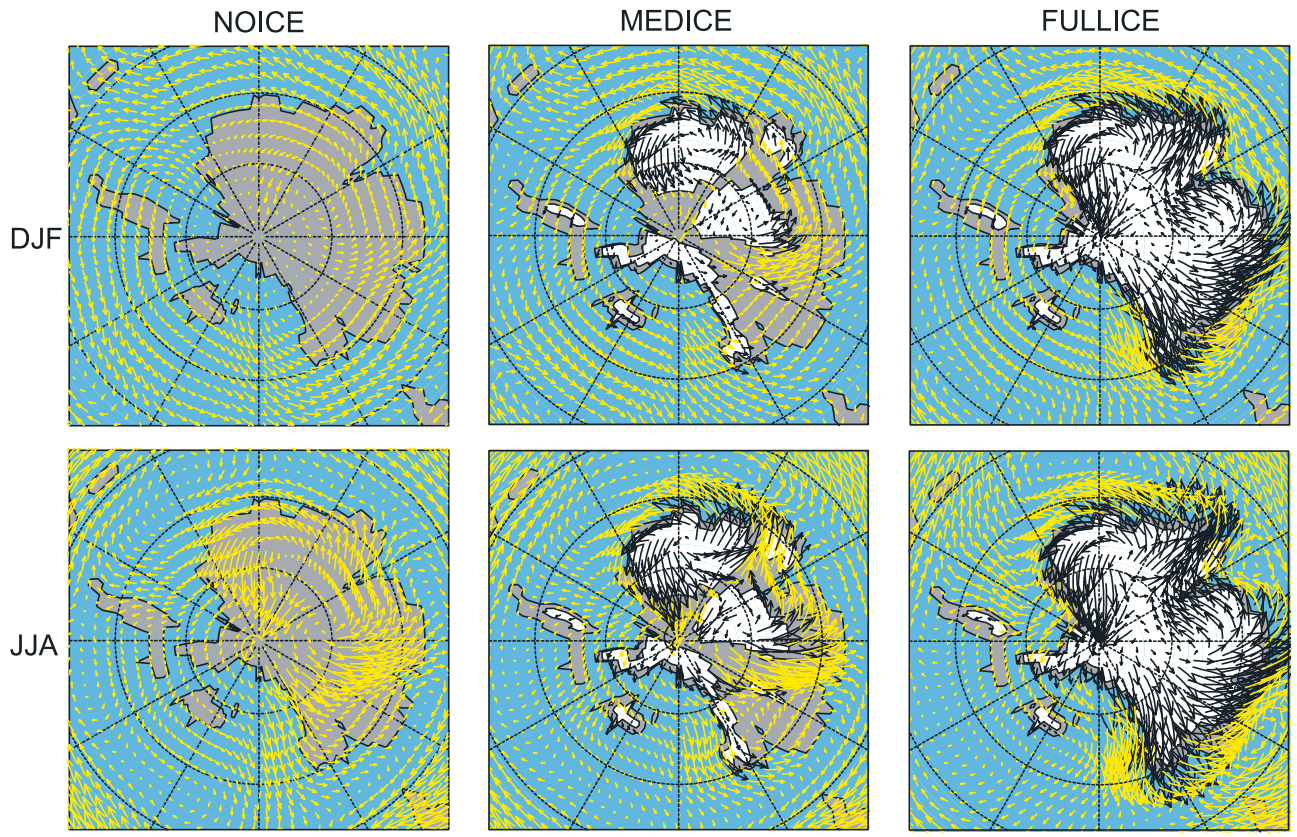

Figure 6. Lowest level (sigma = 0.189) GCM winds during austral summer (top) and winter (bottom) from the three NOICE, MEDICE, and FULLICE simulations, as in Figures 2d and 3. Vector scale length is equivalent to 2° per m s^{-1} of wind velocity. Prescribed ice sheet geometries are shown in white.

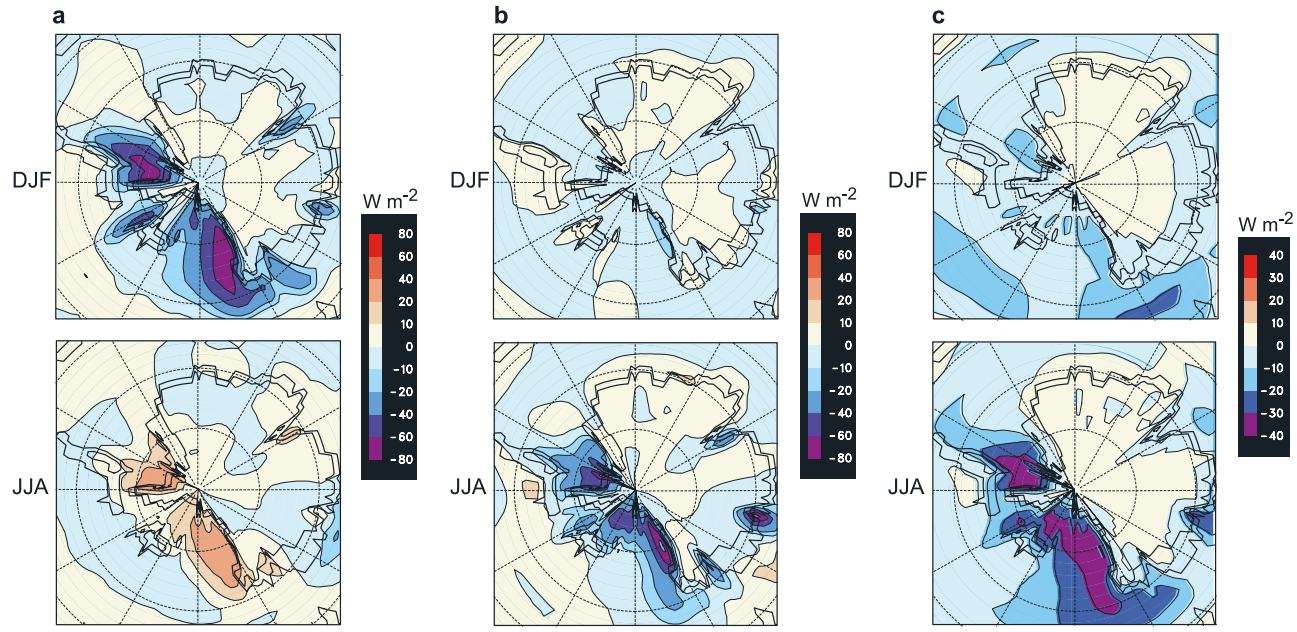

Figure 7. Seasonal differences of (a) net downward radiative flux, (b) upward sensible heat flux, and (c) upward latent heat flux between the maximum, prognostic (FULLICE) case and the minimal, prescribed sea ice case (MINSEAICE). Contour intervals in W m^{-2} are shown to the right of each panel.

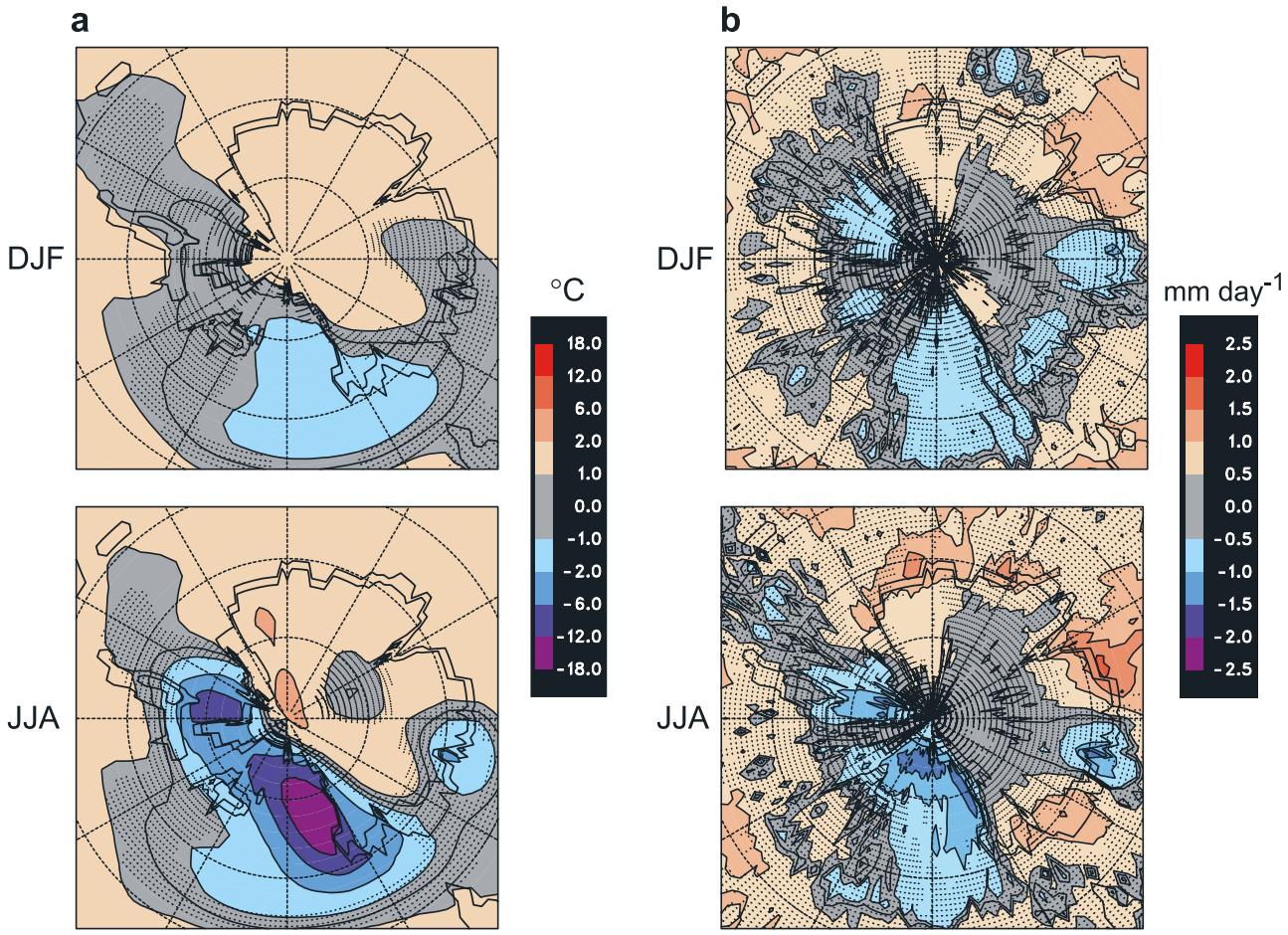

Figure 8. Seasonal differences (MAXSEAICE minus MINSEAICE) in (a) surface (2 m) temperature (°C) and (b) precipitation rate (mm day^{-1}). Differences under nonstippled areas are statistically significant at the 95% confidence level as determined by Student's *t* test.

in the equilibrated ice sheet geometries reflect the sign and strength of the Antarctic sea ice-glaciation feedback. To minimize biases introduced by interannual variability, the ice-driving climatologies are calculated from the last 10 years of the fully equilibrated, 30-year MAXSEAICE and MINSEAICE simulations. As in our prior coupled GCM-ice sheet experiments [*DeConto and Pollard*, 2003a; *DeConto and Pollard*, 2003b], relevant monthly mean meteorological fields used in the calculation of net annual surface mass balance (surface air temperature, total precipitation, and snowfall) are horizontally interpolated and lapse-rate adjusted from the GCM to the finer (40 km) ice sheet grid. A computationally economical degree-day parameterization [*Ritz et al.*, 1997] is used to calculate ablation, accounting for diurnal cycles and refreezing of meltwater, with early springtime melt saturating the winter snowpack before it becomes mobile. Surface mass balance is recalculated every 200 ice sheet model years to account for changing ice-surface elevations. Net annual snow budgets over the MAXSEAICE ice sheet for both sea ice cases are shown in Figure 11. While differences exist around the East Antarctic coastline and over the Transantarctic Mountains, where snowfall rates are at a maximum and variability in precipitation is expected, mass balance over the continental interior and ice sheet nucleation sites are positive and nearly identical in both cases.

[27] The effects of sea ice on snow budgets should be greater for climates closer to the glaciation threshold (i.e., at higher levels of atmospheric CO_2), however, a prior study using the same coupled GCM-ice sheet model and Paleogene boundary conditions showed that the glaciation threshold is about 2.8 × CO_2; well above the CO_2 value required for significant sea ice expansion around an ice-free or even partially glaciated continent (Figure 2). Assuming most major Cenozoic greenhouse gas perturbations occurred at a rate slower than the response time of continental ice sheets ($\sim 10^3$–10^4 years), low CO_2 conditions cold enough for sea ice implies the existence of a continental-scale ice sheet in the Antarctic interior. Therefore we conclude that sea ice was not a likely player in the initiation of ice sheets in the continental interior and probably was not extensive enough to have a significant direct effect on Southern Hemisphere climate until ice caps already covered much of the continent.

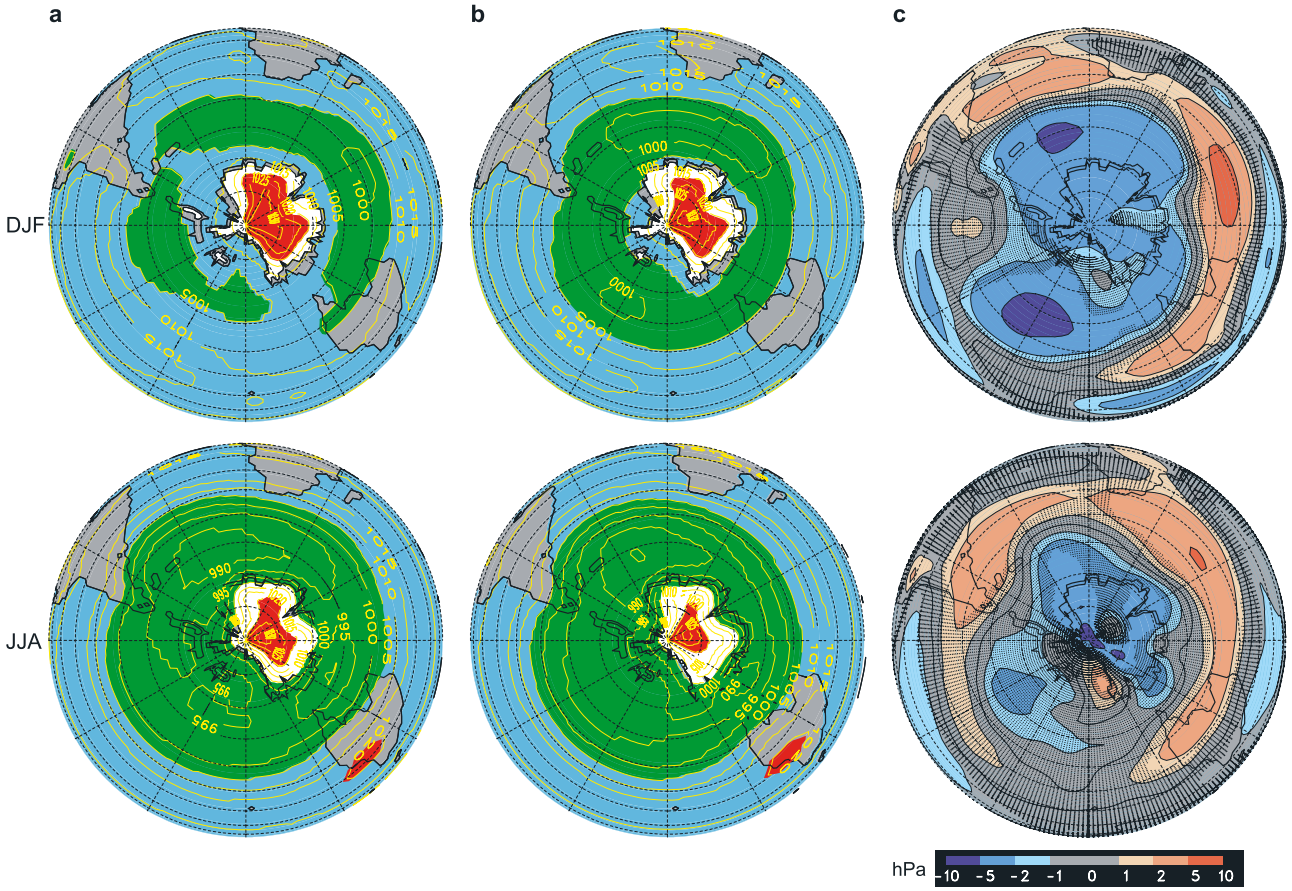

Figure 9. Seasonal sea level pressure in (a) the MINSEAICE case and (b) the MAXSEAICE case. (c) Differences, MAXSEAICE minus MINSEAICE. The contour interval in Figures 9a and 9b is 5 hPa. Contour intervals in Figure 9c are shown below the figure.

[28] The ice sheet model was run for 100,000 years using both mass balance climatologies shown in Figure 11 and identical (MEDICE; Figure 1c) initial ice sheets. The relatively small, initial ice caps allow long spinup times and a comparison of both the rate of glaciation and the final equilibrium ice sheet geometries with minimum versus maximum sea ice. Both simulations follow an almost identical evolution in terms of ice volume, forming a continental-scale EAIS within 20,000 years and reaching equilibrium within 40,000 years. Figure 12 shows fully equilibrated ice sheet geometries and surface elevation in both scenarios. The biggest differences (Figure 12c) occur along the lower latitudes of the Victoria Land margin, where the cooling effects of expansive sea ice in the MAXSEAICE case are greatest while differences in precipitation are relatively small (Figure 8). In the MAXSEAICE case, decreased precipitation in cold, high-elevation areas, such as the Gamburtsev Mountains, reduces ice elevations by ~100 m. Despite these differences in ice sheet geometry, total volume of the equilibrated ice sheets differs by only ~1% (total ice volume in the MINSEAICE and MAXSEAICE cases is 21.20×10^6 and 21.37×10^6 km^3, respectively). Thus at levels of atmospheric CO_2 low enough to allow both ice sheets and sea ice, a growing ice sheet is insensitive to the climatic effects of expanding sea ice.

3. Discussion and Implications of the Results

3.1. Insensitivity of Antarctic Ice Sheets to Sea Ice Extent

[29] Our model results illustrate fundamental differences between the Northern and Southern Hemisphere climate-cryosphere systems. As expected, moisture-ice sheet feedbacks are less important for the Antarctic than the Laurentide. In the Northern Hemisphere, critical areas of sea ice variability and ice sheet growth are generally zonal, within the westerlies, and more easily influenced by changes in upwind moisture sources [*Haug et al.*, 2005]. In contrast, the Antarctic interior is poleward of the sea ice zone and generally upwind of a low-mid level wind regime dominated by southeasterly outflow away from the continental interior. While the growth of sea ice, particularly in the West Antarctic Seaway, removes a regional moisture source for coastal precipitation, the continental interior is not significantly affected. If Paleogene and Neogene source regions of continental moisture were located in low-mid latitudes as suggested by Quaternary isotopic (deuterium excess) studies of interior ice cores [*Stenni et al.*, 2001], early Antarctic ice

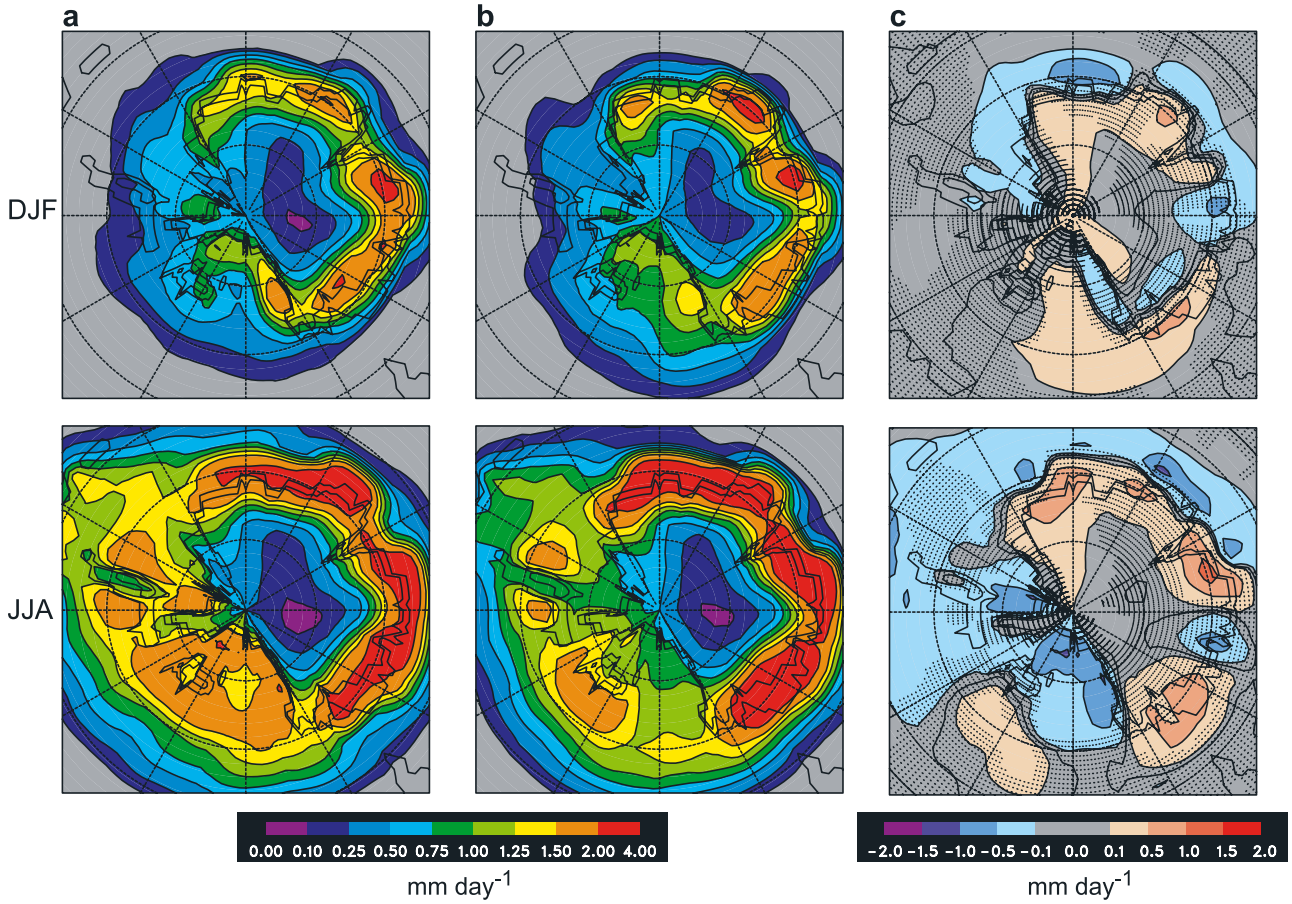

Figure 10. Seasonal snowfall rates in mm day^{-1} for (a) the MINSEAICE case and (b) the MAXSEAICE case. (c) Seasonal differences in snowfall for austral summer (left) and winter (right).

sheets could have been sensitive to changes in tropical SSTs and (Tethyan) gateways. The relative sensitivity of ice sheet evolution to low-latitude versus circum-Antarctic SSTs and sea ice should be tested in future modeling studies.

3.2. Sea Ice-Ice Sheet Feedbacks Relative to Other Forces of Cenozoic Climate Change

[30] Direct, physical (non-CO_2) sea ice feedbacks on Antarctic climate and ice sheet mass balance are much

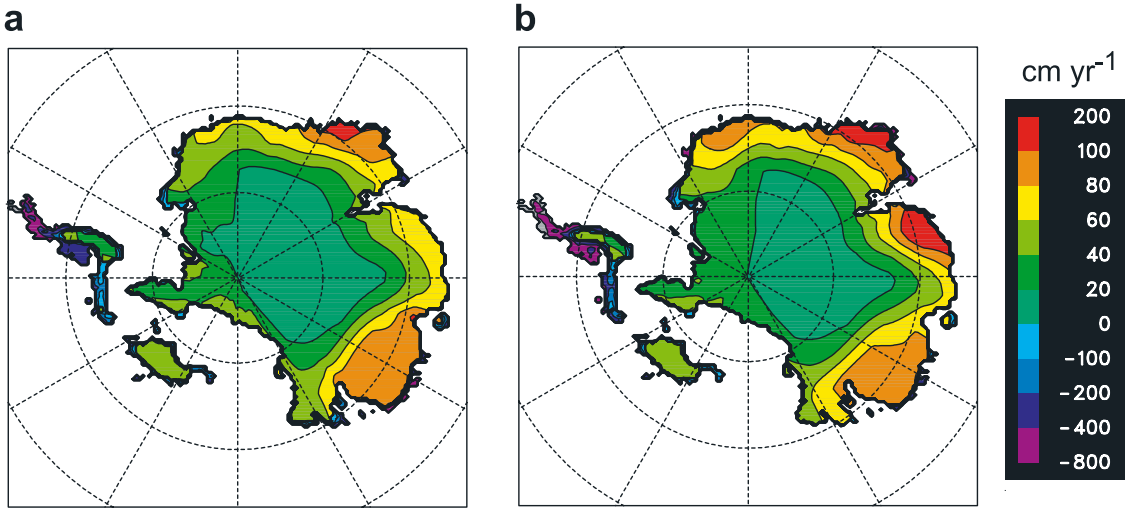

Figure 11. Net annual snow budget over a fully glaciated continent as calculated from meteorological fields in the (a) MINSEAICE and (b) MAXSEAICE GCM simulations.

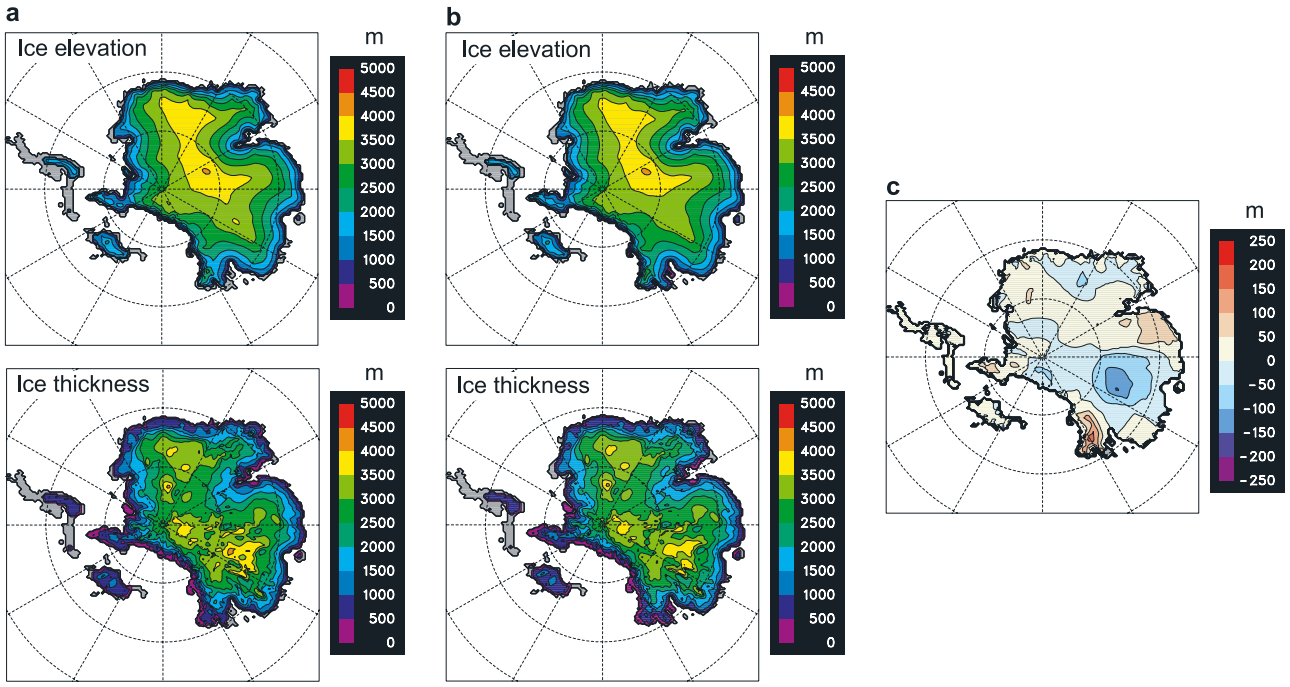

Figure 12. The simulation of an East Antarctic Ice Sheet as simulated by the dynamical ice sheet model for (a) the MINSEAICE case and (b) the MAXSEAICE case. Ice sheet geometry (ice surface elevation (top panels) and ice thickness (bottom panels) are shown after 100,000 years and are fully equilibrated with the forcing climatologies. (c) The difference in ice sheet elevations (MAXSEAICE minus MINSEAICE) shows the net effect of sea ice feedback on ice sheet evolution.

weaker than the albedo and height-mass balance feedbacks shown to be largely responsible for the rapid, nonlinear growth of a Paleogene EAIS in response to a gradual decline in atmospheric CO_2 [*DeConto and Pollard*, 2003a; *DeConto and Pollard*, 2003b; *Pollard and DeConto*, 2005]. The limited climatic effects of Antarctic ice sheet and sea ice expansion on the Northern Hemisphere (Figure 5) also suggests that additional forcings and/or feedbacks not included in our model are required to invoke the dramatic global changes recognized from a wide variety of proxy records, paleoenvironments, and latitudes in the earliest Oligocene [*Prothero et al.*, 2003]. Cenozoic greenhouse gas forcing may provide a reasonable explanation. Antarctic glaciation-CO_2 feedbacks, perhaps triggered by some other mechanism, such as astronomical and/or tectonic forcing, could have contributed to the nonlinear response of the climate system at the Eocene-Oligocene boundary and other intervals of sudden change recognized in Cenozoic proxy records of temperature and ice volume [*DeConto and Pollard*, 2003b; *Zachos and Kump*, 2005]. This notion is generally supported by highly resolved deep-sea records of the Oi-1 transition [*Coxall et al.*, 2005], the ephemeral Mi-1 glaciation [*Zachos et al.*, 2001b], and other climate-cryosphere events through the Paleogene and Neogene [*Zachos et al.*, 2001a], correlated with prolonged orbital periods of low seasonality [*Pälike et al.*, 2007] and perturbations to the carbon cycle recognized in proxy reconstructions of CO_2, carbon isotopes, and changes in the calcium compensation depth of the oceans [*Coxall et al.*, 2005; *Lear et al.*, 2004; *Pagani et al.*, 2005].

3.3. Ice Sheet-Sea Ice-Ocean Feedbacks and Possible Linkages with pCO_2

[31] While we tested sea ice response to a wide range of possible Cenozoic forcings (Table 1), the computational demands imposed by the long spin-up times of ocean general circulation models precluded the use of a coupled atmosphere-ocean GCM (AOGCM) model for the 19 experiments run here. Our slab-ocean component does not include an explicit representation of the deep ocean; however, the dramatic seasonal sea ice expansion in response to ice sheet growth shown in Figure 3 eludes possible linkages between ice sheets, sea ice, thermohaline circulation, and atmospheric CO_2. The simulated cooling and increase in seasonal sea ice and brine rejection likely affected vertical density gradients and stratification of the circum-Antarctic ocean, with probable consequences for the location and magnitude of deep-water formation and the thermohaline component of meridional overturning. Fresh water runoff during times of deglaciation, also lacking in our model, also would have affected circum-Antarctic water column structure. However, any resulting changes in ocean circulation may have had only minimal effects on the Antarctic interior, as suggested by coupled GCM-ice sheet simulations [*DeConto and Pollard*, 2003b], in which imposed changes in poleward ocean heat transport are shown to have only a small effect on Antarctic glacial mass balance.

[32] On the basis of their numerical modeling work, *Mikolajewicz et al.* [1993] and *Huber et al.* [2004] speculated that the indirect influence of Southern Ocean gateways on the marine carbon cycle and atmospheric CO_2 may be

more important to Cenozoic cooling and Antarctic glaciation than the direct, physical effects of changing ocean circulation patterns and ocean heat transport. Here we speculate that ice sheet-sea ice-CO_2 feedbacks involving ventilation rates, overturning, and stratification could also be important. Southern Ocean sea ice has been implicated in the ~80 ppmv range of glacial-interglacial atmospheric CO_2 via its insulating effect on air-sea gas exchange [*Stephens and Keeling*, 2000] and indirectly through stratification and the westerlies' influence on ventilation rates of respired CO_2 [*Toggweiler et al.*, 2006]. While the potential of these mechanisms to affect atmospheric CO_2 remains equivocal [*Archer et al.*, 2003; *Maqueda and Rhamsdorf*, 2002], our simulations do show both expanding sea ice (Figure 3) and dramatic strengthening of the polar easterlies and westerlies (Figure 6) in response to a growing EAIS. Expanding sea ice and increased frontal divergence and upwelling implied by the intensification of the Southern Ocean wind field could have important consequences for air-sea gas exchange and the biological pump [*Broecker*, 1982], possibly contributing to CO_2 drawdown and enhanced cooling at the onset of Cenozoic glaciation events such as Oi-1 [*Zachos and Kump*, 2005].

3.4. Sea Ice and Development of the West Antarctic Ice Sheet

[33] While our results show sea ice-ice sheet feedbacks are not important for the glaciation of East Antarctica, they could have been an important factor in the early development of the West Antarctic Ice Sheet (WAIS) sometime in the Late Cenozoic [*Scherer*, 1991]. In our fixed ice sheet simulations (NOICE, MEDICE, and FULLICE), West Antarctica is presumed to have only limited, small ice caps on the individual islands of the paleo-West Antarctic archipelago. This version of our ice sheet model does not include explicit ice shelves; nor does it account for eustacy in response to a growing ice sheet, so the area of West Antarctica available to accommodate an ice sheet remains small throughout our dynamic ice sheet simulations (Figure 12). At 2 × CO_2, thick, perennial sea ice is wind-driven against the poleward side of West Antarctic islands (Figure 3), in the shallow depths of the West Antarctic Seaway. The climatic conditions capable of supporting thick perennial sea ice are also amenable to ice shelves. This hints at the possibility that floating ice, grounding as parts of the shallow West Antarctic Seaway shoaled during a glacioeustatic fall, could have contributed to the development of the WAIS in a scenario similar to that proposed for the growth of a Barents Sea ice sheet during the last glacial cycle [*Hughes*, 1987].

3.5. Implications for Cenozoic Ice Sheet Reconstructions

[34] The simulated, direct relationship between grounded ice volume and sea ice extent (Figure 2) implies sea ice is representative of the conditions in the continental interior. According to our model results, evidence of extensive, pervasive open water in the Ross Sea sector would suggest reduced grounded ice in the continental interior and evidence of a dynamic ice sheet as proposed for the Pliocene [*Webb and Harwood*, 1991; *Webb et al.*, 1984]. Conversely, proxy evidence of persistent circum-Antarctic sea ice through the Late Cenozoic would suggest a large, stable ice sheet [*Denton et al.*, 1993] because even with elevated atmospheric CO_2, extensive seasonal sea ice would be maintained during all but the warmest orbital periods, provided the East Antarctic interior remained glaciated.

[35] Thick glacial and glacimarine strata from the Sirius Group in the Transantarctic Mountains [*Hambrey et al.*, 2003; *Webb et al.*, 1996; *Wilson et al.*, 1998] and Pagodroma Group in the Prince Charles Mountains in the Lambert Graben region [*Hambrey and McKelvey*, 2000b; *Whitehead et al.*, 2004] reveal processes of Neogene sedimentation with abundant meltwater, high erosion and deposition rates, and a glacial regime warmer than at present. Our model results show that sea ice would have been substantially reduced during deposition of these units. Conversely, cold, polar ice sheets produce little in the way of a sedimentary record and minimal erosional surfaces. In this case, proxy evidence from sea ice related diatoms can be used to infer times of coldest ice [*Armand and Leventer*, 2003; *Whitehead et al.*, 2005]. The oldest sea ice related diatom flora that bears strong similarity to the modern assemblage is reported from late Miocene sediments in a glacial erratic from McMurdo Sound [*Harwood and Bohaty*, 2000], but this distinctive flora is absent or reduced in many Pliocene marine sections, supporting the possibility of reduced glacial ice volume. Glacial and marine sedimentary records to be recovered by the new Antarctic Drilling program (ANDRILL) [*Harwood et al.*, 2006], combined with model results like those shown here, are likely to help resolve the magnitude and timing of Cenozoic Antarctic glacial and climatic variations.

4. Summary and Conclusions

[36] A suite of GCM sensitivity tests with different Antarctic ice sheet configurations, CO_2 concentrations, and a Paleogene (34 Ma) paleogeography shows the influence of EAIS evolution on Southern Ocean surface temperatures, the katabatic wind field, and sea ice extent. While the global boundary conditions used in our simulations represent the world at the time of the Oi-1 glaciation, the results are applicable to other times of large-scale Antarctic glacial advance, like those proposed to have occurred multiple times through the Paleogene and Neogene [*Zachos et al.*, 2001a].

[37] At 2 × CO_2, our model produces little or no sea ice unless a continental-scale ice sheet is already in place. Because 2 × CO_2 is below the simulated level required for rapid glaciation of East Antarctica, we conclude that any positive (cooling) feedbacks associated with expanding sea ice are not necessary for ice sheet initiation and glacial advance on East Antarctica.

[38] While the growth of sea ice is shown to have a dramatic climatic effect over the sea ice zone and some parts of the Antarctic coastline, the mass balance effects on a partially glaciated continental interior are small. Thus once an ice sheet is established and is large enough to alter Southern Ocean climate to the extent that significant sea ice begins to form, the ice sheet itself is relatively insensitive to the climate effects imposed by the expanding sea ice.

[39] From a modeling perspective, physical sea ice-ice sheet feedbacks appear less important to Cenozoic variability of Antarctic ice sheets than other internal climate system feedbacks. The simulated effects of ice sheets and sea ice expansion on the Southern Ocean wind field and SSTs suggest linkages between grounded ice, sea ice, and the marine carbon cycle may have contributed to fluctuations in CO_2 [*Crowley and Zachos*, 1999; *Lear et al.*, 2004] and the nonlinear behavior of the climate system recognized in Cenozoic proxy climate records [*Coxall et al.*, 2005; *Pälike et al.*, 2007; *Zachos et al.*, 2001a].

[40] While not a requirement for East Antarctic glaciation in the Paleogene, the development of circum-Antarctic sea ice might have contributed to the glaciation of West Antarctica sometime in the Neogene. The formation of extensive seasonal and perennial sea ice in response to a growing EAIS would have cooled the lower latitudes of the West Antarctica archipelago, possibly increasing net annual accumulation. While ice shelves are not explicitly represented here, thick perennial sea ice predicted at times in the shallow seaway separating East and West Antarctica, could have facilitated ice shelf development, further aiding WAIS growth.

[41] The simulated response of Southern Ocean sea ice to Antarctic ice volume suggests proxy records of sea ice extent may be indicative of climatic and glacial conditions in the continental interior. Therefore reconstructions of Southern Ocean sea ice may provide some insight as to the long-term stability of Antarctic ice sheets.

[42] **Acknowledgments.** This research was funded by the US National Science Foundation under awards ATM 0513402/0513421 and ANT-034248.

References

Andreas, E. L., and B. Murphy (1986), Bulk transfer coefficients for heat and momentum over leads and polynas, *J. Phys. Oceanogr.*, *16*, 1875–1883.

Archer, D. E., P. A. Martin, J. Milovich, V. Brovkin, G. K. Plattner, and C. Ashendel (2003), Model sensitivity in the effect of Antarctic sea ice and stratification on atmospheric pCO_2, *Paleoceanography*, *18*(1), 1012, doi:10.1029/2002PA000760.

Armand, L. K. (2000), An ocean of ice—Advances in the estimation of past sea-ice in the Southern Ocean, *GSA Today*, *10*, 1–7.

Armand, L. K., and A. Leventer (2003), Palaeo sea ice distribution—Reconstruction and palaeoclimatic significance, in *Sea Ice: Physics, Biology, Chemistry and Biology*, edited by D. Thomas and G. Dieckmann, pp. 333–372, Blackwell Sci., Malden, Mass.

Bamber, J. A., and R. A. Bindschadler (1997), An improved elevation dataset for climate and ice-sheet modelling: Validation with satellite imagery, *Ann. Glaciol.*, *25*.

Billups, K., and D. P. Schrag (2002), Paleotemperatures and ice volume of the past 27 Myr revisited with paired Mg/Ca and O-18/O-16 measurements on benthic foraminifera, *Paleoceanography*, *17*(1), 1003, doi:10.1029/2000PA000567.

Billups, K., and D. P. Schrag (2003), Application of benthic foraminiferal Mg/Ca ratios to questions of Cenozoic climate change, *Earth Planet. Sci. Lett.*, *209*, 181–195.

Bohaty, S. M., R. P. Scherer, and D. M. Harwood (1998), Lower Pleistocene diatom biostratigraphy of the CRP-1 drillcore, *Terra Antarctica*, *Sci. Result. Cape Roberts Drill. Proj.*, *5*, 431–454.

Broecker, W. S. (1982), Glacial to interglacial changes in ocean chemistry, *Prog. Oceanogr.*, *11*, 151–197.

Bromwich, D. H., B. Chen, and K. M. Hines (1998a), Global atmospheric impacts induced by year-round open water adjacent to Antarctica, *J. Geophys. Res.*, *103*, 11,173–11,189.

Bromwich, D. H., B. Chen, K. M. Hines, and R. I. Cullather (1998b), Global atmospheric responses to Antarctic forcing, *Ann. Glaciol.*, *27*, 521–527.

Brotchie, J. F., and R. Sylvester (1969), On crustal flexure, *J. Geophys. Res.*, *74*, 5240–5252.

Carleton, A. M. (1989), Antarctic sea-ice relationships with indices of the atmospheric circulation of the southern hemisphere, *Clim. Dyn.*, *3*(CA), 207–220.

Carleton, A. M. (2003), Atmospheric teleconnections involving the Southern Ocean, *J. Geophys. Res.*, *108*(C4), 8080, doi:10.1029/2000JC000379.

Cooke, D. W., and J. D. Hays (1982), Estimates of Antarctic Ocean seasonal sea-ice cover during glacial intervals, in *Antarctic Geoscience*, edited by C. Craddock, pp. 1017–1025, Union of Wisconsin Press, Madison.

Coxall, H. K., P. A. Wilson, H. Pälike, C. Lear, and J. Backman (2005), Rapid stepwise onset of Antarctic glaciation and deeper calcite compensation in the Pacific Ocean, *Nature*, *433*, 53–57.

Crosta, X., J. J. Pichon, and L. H. Burckle (1998), Application of modern analog technique to marine Antarctic diatoms: Reconstruction of maximum sea-ice extent at the Last Glacial Maximum, *Paleoceanography*, *13*, 284–297.

Crowley, T. J., and J. Zachos (1999), Comparison of zonal temperature profiles for past warm time periods, in *Warm Climates in Earth History*, edited by B. T. Huber, S. L. Wing, and K. G. MacLeod, pp. 50–76, Cambridge Univ. Press, New York.

DeConto, R. M., and D. Pollard (2003a), A coupled climate-ice sheet modeling approach to the early Cenozoic history of the Antarctic ice sheet, *Palaeogeogr., Palaeoclimatol., Palaeoecol.*, *198*, 39–53.

DeConto, R. M., and D. Pollard (2003b), Rapid Cenozoic glaciation of Antarctica induced by declining atmospheric CO_2, *Nature*, *421*, 245–249.

Denton, G. H., D. E. Sugden, D. R. Marchant, B. L. Hall, and T. L. Wilch (1993), East Antarctic ice sheet sensitivity to Pliocene climatic change from a Dry Valleys perspective, *Geogr. Ann.*, *75*, 155–204.

Fahbach, E., G. Rohardt, M. Schroder, and V. Strass (1994), Transport and structure of the Weddell Gyre, *Ann. Geophys. - Atmos., Hydrospheres, Space Sci.*, *12*, 840–855.

Flato, G. M., and W. D. Hibler (1990), On a simple sea-ice dynamics model for climate studies, *Ann. Glaciol.*, *14*.

Flato, G. M., and W. D. Hibler (1992), Modeling pack ice as a cavitating fluid, *J. Phys. Oceanogr.*, *22*, 626–651.

Fletcher, J. O. (1969), Ice extent in the southern oceans and its relation to world climate, *J. Glaciol.*, *15*, 417–427.

Gersonde, R., X. Crosta, A. Abelmann, and L. Armand (2005), Sea-surface temperature and sea-ice distribution of the Southern Ocean at the EPILOG Last Glacial Maximum—A circum-Antarctic view based on siliceous microfossil records, *Quat. Sci. Rev.*, *24*, 496–869.

Gloerson, P. (1995), Modulation of hemispheric sea-ice cover by ENSO events, *Nature*, *373*, 503–506.

Hambrey, M. J., and B. C. McKelvey (2000a), Major Neogene fluctuations of the East Antarctic Ice Sheet: Stratigraphic evidence from the Lambert Glacier region, *Geology*, *28*, 887–890.

Hambrey, M. J., and B. C. McKelvey (2000b), Neogene fjordal sedimentation on the western margin of the Lambert Graben, East Antarctica, *Sedimentology*, *43*, 577–607.

Hambrey, M. J., P. N. Webb, D. M. Harwood, and L. A. Krissek (2003), Neogene glacial record from the Sirius Group of the Shackleton Glacier region, central Transantarctic Mountains, Antarctica, *Geol. Soc. Am. Bull.*, *115*, 994–1015.

Harvey, L. D. D. (1988), Development of a sea ice model for use in zonally averaged energy balance models, *J. Clim.*, *1*, 1221–1238.

Harwood, D., and S. Bohaty (2000), Marine diatom assemblages from Eocene and younger erratics, McMurdo Sound, Antarctica, in *Paleobiology and Paleoenvironments of Eocene Fossiliferous Erratics, McMurdo Sound, East Antarctica*, edited by J. D. Stilwell and R. M. Feldmann, pp. 73–98, AGU, Washington, D. C.

Harwood, D. M., A. McMinn, and P. G. Quilty (2000), Diatom ages of Sørsdal Formation, Vestfold Hills, Antarctica, *Antarct. Sci.*, *14*, 443–462.

Harwood, D., R. Levy, J. Cowie, F. Florindo, T. Naish, R. Powell, and A. Pyne (2006), Deep drilling with the ANDRILL Program in Antarctica, *Sci. Drill.*, *3*, 43–45.

Haug, G. H., et al. (2005), North Pacific seasonality and the glaciation of North America 2.7 million years ago, *Nature*, *433*, 821–825.

Hay, W. W., R. M. DeConto, C. N. Wold, K. M. Wilson, S. Voigt, M. Schulz, A. Wold-Rossby, W.-C. Dullo, A. B. Ronov, and A. N. Balukhovsky (1999), An alternative global Cretaceous paleogeography, in *The Evolution of Cretaceous/Ocean Climate Systems*, edited by E. Barrera and C. Johnson, pp. 1–48, Geol. Soc. Am., Boulder.

Hibler, W. D. (1979), A dynamic thermodynamic sea ice model, *J. Phys. Oceanogr.*, *9*, 815–846.

Holbourn, A., W. Kuhnt, M. Schulz, and H. Erlrnkeuser (2005), Impacts of orbital forcing and atmospheric carbon dioxide on Miocene ice-sheet expansion, *Nature*, *438*, 483–487.

Houghton, J. T., G. J. Jenkins, and J. J. Ephraums (Eds.) (1990), *Climate Change: The IPCC Scientific Assessment*, 365 pp., Cambridge Univ. Press, New York.

Huber, M., H. Brinkhuis, C. E. Stickley, K. Doos, A. Sluijs, J. Warnaar, S. A. Schellenberg, and G. L. Williams (2004), Eocene circulation of the Southern Ocean: Was Antarctica kept warm by subtropical waters?, *Paleoceanography*, *19*, PA4026, doi:10.1029/2004PA001014.

Hughes, T. J. (1987), The marine-ice transgression hypothesis, *Geogr. Ann.*, *69*, 237–250.

Huybrechts, P. (1990), A 3-D model for the Antarctic ice sheet: A sensitivity study on the glacial-interglacial contrast, *Clim. Dyn.*, *5*, 79–92.

Huybrechts, P. (1993), Glaciological modelling of the late Cenozoic East Antarctic ice sheet: Stability or dynamism?, *Geogr. Ann.*, *75*, 221–238.

Ingram, W. J., C. A. Wilson, and J. F. B. Mitchell (1989), Modeling climate change: An assessment of sea ice and surface albedo feedbacks, *J. Geophys. Res.*, *94*, 8609–8622.

Jeffries, M. O. (1998), *Antarctic Sea Ice: Physical Processes, Interactions, and Variability*, 407 pp., AGU, Washington, D. C.

King, J. C., and J. Turner (1997), *Antarctic Meteorology and Climatology*, 409 pp., Cambridge Univ. Press, New York.

Lear, C. H., H. Elderfield, and P. A. Wilson (2000), Cenozoic deep-sea temperatures and global ice volumes from Mg/Ca in benthic foraminiferal calcite, *Science*, *287*, 269–272.

Lear, C. H., Y. Rosenthal, H. K. Coxall, and P. A. Wilson (2004), Late Eocene to early Miocene ice-sheet dynamics and the global carbon cycle, *Paleoceanography*, *19*, PA4015, doi:10.1029/2004PA001039.

Ledley, T. S. (1991), Snow on sea ice: Competing effects in shaping climate, *J. Geophys. Res.*, *96*, 17,195–17,208.

Liu, J., J. A. Curry, and D. Martinson (2004), Interpretation of recent Antarctic sea ice variability, *Geophys. Res. Lett.*, *31*, LO2205, doi:10.1029/2003GL018732.

Liu, J. P., D. G. Martinson, X. J. Yuan, and D. Rind (2002), Evaluating Antarctic sea ice variability and its teleconnections in global climate models, *Int. J. Climatol.*, *22*, 885–900.

Liu, J. P., G. A. Schmidt, D. G. Martinson, D. Rind, G. Russell, and X. J. Yuan (2003), Sensitivity of sea ice to physical parameterizations in the GISS global climate model, *J. Geophys. Res.*, *108*(C2), 3053, doi:10.1029/2001JC001167.

Lubin, D., B. Chen, D. H. Bromwich, R. C. J. Somerville, W. H. Lee, and K. M. Hines (1998), The impact of Antarctic cloud radiative properties on a GCM climate simulation, *J. Clim.*, *11*, 447–462.

Mahood, A. D., and J. A. Barron (1996), Late Pliocene diatoms in a diatomite from Prydz Bay, East Antarctica, *Micropaleontology*, *42*, 285–302.

Maqueda, M. A. M., and S. Rhamsdorf (2002), Did Antarctic sea-ice expansion cause glacial CO_2 decline?, *Geophys. Res. Lett.*, *29*(1), 1011, doi:10.1029/2001GL013240.

Mikolajewicz, U., E. Maier-Reimer, T. J. Crowley, and K.-Y. Kim (1993), Effect of Drake and Panamanian gateways on the circulation of an ocean model, *Paleoceanography*, *8*, 409–426.

Miller, K. G., R. G. Fairbanks, and G. S. Mountain (1987), Tertiary oxygen isotope synthesis, sea level history, and continental margin erosion, *Paleoceanography*, *1*, 1–20.

Oglesby, R. J. (1989), A GCM study of Antarctic Glaciation, *Clim. Dyn.*, *3*, 135–156.

Pagani, M., J. C. Zachos, K. H. Freeman, B. Tipple, and S. M. Bohaty (2005), Marked decline in atmospheric carbon dioxide concentrations during the Paleogene, *Science*, *309*, 600–603.

Pälike, H., R. D. Norris, J. O. Herrle, P. A. Wilson, H. K. Coxall, C. H. Lear, N. J. Shackleton, A. Tripati, and B. S. Wade (2007), The heartbeat of the Oligocene climate system, *Nature*, *314*, 1894–1897.

Parkinson, C. L. (1998), Length of sea ice season in the Southern Ocean, in *Antarctic Sea Ice: Physical Processes, Interactions, and Variability*, edited by M. O. Jeffries, pp. 173–186, AGU, Washington, D. C.

Parkinson, R., D. Rind, R. Healy, and D. Martinson (2001), The impact of sea ice concentration accuracies on climate model simulations with the GISS GCM, *J. Clim.*, *14*, 2606–2623.

Pollard, D. (2000), Comparisons of ice-sheet surface mass budgets from Paleoclimate Modeling Intercomparison Project (PMIP) simulations, *Global Planet. Change*, *24*, 79–106.

Pollard, D., and R. M. DeConto (2005), Hysteresis in Cenozoic Antarctic Ice Sheet variations, *Global Planet. Change*, *45*, 9–21.

Pollard, D., and S. L. Thompson (1994), Sea-ice dynamics and CO_2 sensitivity in a global climate model, *Atmos.-Ocean*, *32*, 449–467.

Pollard, D., and S. L. Thompson (1997), Driving a high-resolution dynamic ice-sheet model with GCM climate: Ice sheet initiation at 116,000 BP, *Ann. Glaciol.*

Prentice, M. L., and R. K. Mathews (1991), Tertiary ice sheet dynamics: The snow gun hypothesis, *J. Geophys. Res.*, *96*, 6811–6827.

Prothero, D. R., L. C. Ivany, and E. A. Nesbitt (Eds.) (2003), *From Greenhouse to Icehouse: The Marine Eocene–Oligocene Transition*, 541 pp., Columbia Univ. Press, New York.

Rind, D., R. Healy, C. Parkinson, and D. Martinson (1995), The role of sea ice in $2 \times CO_2$ climate model sensitivity. Part I: The total influence of sea-ice thickness and extent, *J. Clim.*, *8*, 449–463.

Ritz, C., A. Fabre, and A. Letreguilly (1997), Sensitivity of a Greenland ice sheet model to ice flow and ablation parameters: Consequences for the evolution through the last climate cycle, *Clim. Dyn.*, *13*, 11–24.

Sayag, R., E. Tziperman, and M. Ghil (2004), Rapid switch-like sea ice growth and land ice-sea ice hysteresis, *Paleoceanography*, *19*, PA1021, doi:10.1029/2003PA000946.

Scherer, R. P. (1991), Quaternary and Tertiary mircofossils from beneath Ice Stream B—Evidence for a dynamic West Antarctic Ice Sheet history, *Global Planet. Change*, *90*, 395–412.

Semtner, A. J. (1976), A model for the thermodynamic growth of sea ice in numerical model investigations of climate, *J. Phys. Oceanogr.*, *6*, 379–389.

Shin, S.-I., Z. Liu, B. Otto-Bliesner, J. E. Kutzbach, and S. J. Vavrus (2003), Southern Ocean sea-ice control of the glacial North Atlantic thermohaline circulation, *Geophys. Res. Lett.*, *30*(2), 1096, doi:10.1029/2002GL015513.

Simmonds, I., and W. F. Budd (1991), Sensitivity of the Southern Hemisphere circulation to leads in the Antarctic ice pack, *Q. J. R. Meteorol. Soc.*, *117*, 1003–1024.

Simmonds, I., and T. H. Jacka (1995), Relationships between the interannual variability of Antarctic sea ice and the Southern Oscillation, *J. Clim.*, *8*, 637–647.

Stenni, B., V. Masson-Delmotte, S. Johnsen, J. Jouzel, A. Longinelli, E. Monnin, R. Rothlisberger, and E. Selmo (2001), An oceanic cold reversal during the last deglaciation, *Science*, *293*, 2074–2077.

Stephens, B. B., and R. F. Keeling (2000), The influence of Antarctic sea ice on glacial–interglacial CO_2 variations, *Nature*, *404*, 171–174.

Sturm, M., K. Morris, and R. Massom (1998), The winter snow cover of the west antarctic pack ice: Its spatial and temporal variability, in *Antarctic Sea Ice: Physical Processes, Interactions and Variability*, edited by M. O. Jeffries, pp. 1–19, AGU, Washington, D. C.

Thompson, S. L., and D. Pollard (1997), Greenland and Antarctic mass balances for present and doubled atmospheric CO_2 from the GENESIS Version-2 Global Climate Model, *J. Clim.*, *10*, 871–900.

Toggweiler, J. R., J. L. Russell, and S. R. Carson (2006), Midlatitude westerlies, atmospheric CO_2, and climate change during the ice ages, *Paleoceanography*, *21*, PA2005, doi:10.1029/2005PA001154.

Washington, W. M., and G. A. Meehl (1996), High-latitude climate change in a global coupled ocean–atmosphere–sea ice model with increased atmospheric CO_2, *J. Geophys. Res.*, *101*, 12,795–12,801.

Weatherly, J. W. (2004), Sensitivity of Antarctic precipitation to sea ice concentrations in a general circulation model, *J. Clim.*, *17*, 3214–3223.

Webb, P.-N., and D. M. Harwood (1991), Late Cenozoic glacial history of the Ross Embayment, Antarctica, *Quat. Sci. Rev.*, *10*, 215–223.

Webb, P.-N., D. M. Harwood, M. G. C. Mabin, and B. C. McKelvey (1996), A marine and terrestrial Sirius group succession, middle Beardmore glacier Queen Alexandra range, Transantarctic mountains, Antarctica, *Mar. Micropaleontol.*, *27*, 273–297.

Webb, P.-N., D. M. Harwood, B. C. McKelvey, J. H. Mercer, and L. D. Stott (1984), Cenozoic marine sedimentation and ice-volume variation on the East Antarctic Craton, *Geology*, *12*, 287–291.

Whitehead, J. M., and S. M. Bohaty (2003), Pliocene summer sea surface temperature reconstruction using silicoflagellates from Southern Ocean Site 1165, *Paleoceanography*, *18*(3), 1075, doi:10.1029/2002PA000829.

Whitehead, J. M., D. M. Harwood, B. C. McKelvey, M. J. Hambrey, and A. McMinn (2004), Diatom biostratigraphy of the Cenozoic glaciomarine Pagodroma Group, northern Prince Charles Mountains, East Antarctica, *Aust. J. Earth Sci.*, *51*, 521–547.

Whitehead, J. M., P. G. Quilty, D. M. Harwood, and A. McMinn (2001), Early Pliocene palaeoenvironmental history of the Sørsdal Formation, Vestfold Hills, based on diatom data, *Mar. Micropaleontol.*, *41*, 125–152.

Whitehead, J. M., S. Wotherspoon, and S. M. Bohaty (2005), Minimal Antarctic sea ice during the Pliocene, *Geology*, *33*, 137–140.

Wilson, G. S., D. M. Harwood, R. A. Askin, and R. H. Levy (1998), Late Neogene Sirius Group Strata in Reedy Valley: A multiple resolution record of climate, ice sheet and sea-level events, *J. Glaciol.*, *44*, 437–447.

Winter, D. M., and D. M. Harwood (1997), Integrated diatom biostratigraphy of Late Neogene drillcores in Southern Victoria Land and correlation to Southern Ocean records, in *The Antarctic Region: Geological Evolution and Processes*, edited by C. A. Ricci, pp. 895–992, Siena.

Wu, X. G., I. Simmonds, and W. F. Budd (1996), Southern Hemisphere climate system recovery from 'instantaneous' sea ice removal, *Q. J. R. Meteorol. Soc.*, *122*, 1501–1520.

Zachos, J., and L. Kump (2005), Carbon cycle feedbacks and the initiation of Antarctic glaciation in the earliest Oligocene, *Global Planet. Change*, *47*, 51–66.

Zachos, J., M. Pagani, L. Sloan, and E. Thomas (2001a), Trends, rhythms, and aberrations in global climate 65 Ma to present, *Science*, *292*, 686–693.

Zachos, J. C., N. J. Shackleton, J. S. Revenaugh, H. Palke, and B. Flower (2001b), Climate response to orbital forcing across the Oligocene-Miocene boundary, *Science*, *292*, 274–278.

Zwally, J. H., J. C. Comiso, C. L. Parkinson, D. J. Cavalieri, and P. Gloerson (2002), Variability of Antarctic sea ice 1979–1998, *J. Geophys. Res.*, *107*(C5), 3041, doi:10.1029/2000JC000733.

R. DeConto, Department of Geosciences, University of Massachusetts, Amherst, MA 01003, USA. (deconto@geo.umass.edu)

D. Harwood, Department of Geosciences, University of Nebraska-Lincoln, Lincoln, NE 68588-0340, USA.

D. Pollard, Earth and Environmental Systems Institute, Pennsylvania State University, University Park, PA 16802, USA.